Journal of Medical Phyto Research

Volume 1

June, 2018

ISSN: 2577-6541

FUNDING FOR ALL RESEARCH PROVIDED BY BOMI™

Table of Contents:

Volume 1, Article 1; Pages 3-9 Doi: 10.31013/2002a

A low osmolarity rehydration solution that helps chemo patients

D. Cushing[1]* & B. Joseph[1]

[1]: Peak Health Center, Los Gatos, CA

*For inquiries, email corresponding author at donish@peakhealth.center

Recieved: March 18, 2018

Accepted: March 24, 2018

Published: April 2, 2018

Citation: Cushing, C., Joseph, B. (2018). A low osmolarity rehydration solution that helps chemo patients. Retrieved from https://doi.org/10.31013/2002a

Abstract

Prior research using oral rehydration solutions (ORS) have focused primarily on diarrhea secondary to infectious diseases such as cholera. We evaluated the efficacy of supplying oral rehydration solution (ORS) to patients undergoing chemotherapy. Patients undergoing one of four chemotherapy treatments (CAF, EC, FOLFIRI, or IFL), in one of eleven hospitals, with HDI scores largely representative of the global population (Range: 0.48-0.89), were divided semi-randomly into two groups. Patients in the test group received a low-osmolarity oral rehydration solution powder, and instructed to consume it with water. Patients in the control group did not get the rehydration solution. Return hospital visits were tallied for both groups during the first three months of treatment. Mean return visits per hospital, per treatment, were calculated for each group. A *t*-test for independent samples was conducted on these data points. Welch's *t* was used to make corrected group comparisons between the groups. It found a significant difference in monthly return visit rate between the control group ($M = 4.35$, $SD = 0.61$) and the test group ($M = 0.94$, $SD = 0.18$), $t(23.386) = 24.5$, $p < .001$, $d = 7.58$. The effect size of this difference was remarkably large. Patients who had access to the ORS had return visit rates that were less than 25% of those who did not. This reduction in hospital visits demonstrates that the medical use of appropriate ORS can be used as a supplement treatment for chemotherapy patients.

The deleterious health effects of dehydration cannot be understated (El-Sharkawy, Sahota, & Lobo, 2015). Oral Rehydration Solutions (ORS) were established as a cornerstone of therapy in the 1970's to treat patients with life-threatening dehydration that results from diarrhea, especially from cholera (Binder, Brown, Ramakrishna, & Young 2014). ORS has been repeatedly shown to be an efficacious treatment for cholera-induced diarrhea (Ververs & Narra, 2017; Kühn et al., 2014; Okeke et al., 2005), as well as diarrhea from other cholera-like sources (Gill et al., 2013; Qadri, Svennerholm, Faruque, & Sack, 2005). However, diarrhea can result from noncommunicable diseases as well.

One of the biggest current global health concerns is cancer. Cancer is expected to become a leading cause of morbidity and mortality across all major regions of the

world in the next few decades (Jaspers et al., 2015; Jemal et al., 2011; Ferlay et al., 2008). Common treatment regimens for cancer include some form of chemotherapy. This drug-combination therapy prevents tumor cells from growing or reproducing, and simultaneously starves them of nutrients needed to survive (Muchmore & Wanebo, 2008). During treatment, collateral damage to vital endogenous processes abounds, and results in the destruction of cells, hormones, and enzymes, causing nausea, vomiting, and diarrhea. It can also cause adverse interactions with appetite regulating mediators in the hypothalamus (Sinno et al., 2010). This results in a disinclination to consume water or food, which exacerbates dehydration and leads to a slower, more painful recovery (Daly et al., 2016; Sullivan et al., 2018). Understandably, rehospitalization rates during chemotherapy treatments are very high (Kelly, Cajas, Baumgartner, & Lowy, 2018; Martin et al., 2016; Ang et al., 2015). To date, no study has determined the effiacy of using ORS to treat chemotherapy patients.

Method:

We developed a proprietary low-osmolarity ORS formulation, which we call R^3, based on the World Health Organization (WHO) low osmolarity salts, that replaces water and electrolytes lost through diarrhea, vomiting, and sweating. The present study tested whether administering R^3 to patients undergoing chemotherapy treatments could reduce the rates of rehospitalization during treatment.

Setting

Data were gathered between March, 2016 and August, 2016 from 11 hospitals in 10 countries across Africa, Asia, and Europe. The Human Development Index (HDI) of these countries had a range and distribution generally representative of the global population (Range: 0.48 - 0.89). The hospitals that supplied data, and their respective countries' HDI were: National Oncology Centre, Baku, Azerbaijan (HDI: 0.75), Chonburi Cancer Hospital, Chonburi, Thailand (HDI: 0.73), Gaborone Private Hospital, Gaborone, Botswana (HDI: 0.70), Sir Thutob Namgyal Memorial Hospital, Gangtok, Bhutan (HDI: 0.61), Khartoum Oncology Centre, Khartoum, South Sudan (HDI: 0.48), Lakeshore Cancer Center, Lagos, Nigeria (HDI: 0.51), Lampang Cancer Hospital, Lampang, Thailand (HDI: 0.73), Cancer Diseases Hospital, Lusaka, Zambia (HDI: 0.59), Léon-Bérard Cancer Center, Lyon, France (HDI: 0.89), Texas Cancer Centre, Nairobe, Kenya (HDI: 0.55), and Mount Miriam Cancer Hospital, Pulau Pinang, Malaysia (HDI: 0.78).

Implementation

This study was funded by the IARC working group on cancer prevention. All patients whose data were collected were briefed on the purpose of the study and consented to having their data used. The number of return hospital visits during the first three months of treatment were tallied for use as the dependent variable. We anonymized the by-patient data, and received total rehospitalization rates per hospital per chemotherapy treatment

ORS was hypothesized to relieve the suffering of the chemotherapy patients, so we withheld ORS from only as many patients as needed to provide sufficient statistical strength for analysis. Patients (n = 798) were assigned semi-randomly to either the control group (n = 150) or the ORS group (n = 648). In the control group, patients were sent home after treatment. In the ORS group, during their first chemotherapy visit, patients were given five kilograms of R^3. This formulation has an osmolarity of 172 mOms/L, and contained an organic lemon-lime flavoring to make it more palatable. Patients were instructed to mix thirteen and a half grams for every twelve ounces of water, and to drink that solution four times daily. In the unlikely event that patients consumed all of their ORS powder, additional ORS powder was supplied during the next hospital visit.

Patients' data were collected if they were undergoing one of four chemotherapy treatment types: EC, CAF, IFL, or FOLFIRI. These chemotherapy treatments are administered in hospitals globally. Of the patients in the control group, 29 received CAF, 44 received EC, 41 received FOLFIRI, and 36 received IFL. Of the patients in the ORS group, 123 received CAF, 198 received EC, 211 received FOLFIRI, and 116 received IFL.

Data Analysis

In all but three hospitals, data were recorded for two chemotherapy treatment types. In one hospital (Léon-Bérard Cancer Center in Lyon, France), data were gathered for three types (EC, CAF, and FOLFIRI). In two hospitals (National Oncology Centre in Baku, Azerbaijan, and Sir Thutob Namgyal Memorial Hospital in Gangtok, Bhutan), data were gathered for one type (CAF). In every hospital, for each chemotherapy treatment studied, patients were assigned to both the control and the ORS group. (For

patient counts per chemotherapy treatment type per hospital, see Table 1.)

To make a comparison between patients in the control group and those in the ORS group, we sought a strategy that would provide the fairest compromise between sufficiently valuing and weighting regionally specific data from hospitals that had fewer patients, as well as higher-granularity data provided by hospitals that could treat greater numbers of patients and provide more types of chemo treatments. Conveniently, the hospitals that gave us data for only one chemo treatment had fewer patients receiving that treatment. The hospital that provided three types of chemo treatments had more patients receiving each of those treatments. Thus, we aggregated patients' return visit data into means per chemo treatment per hospital. This resulted in 21 aggregated means per group. We divided these means by three to represent an average monthly visit rate.

We conducted a *t*-test for independent samples on the aggregated hospital data to determine whether there was a significant effect of the ORS on the monthly return visit rate. This was the primary aim of our study.

Further comparisons between chemotherapy treatments were conducted, however they relied on variance that was estimated from 5-6 data points per condition per group. Low degrees of freedom provided by these data have an extremely low power of 1-ß = .22. Furthermore, not all hospitals provided data on the same chemotherapy treatment types. As such, these comparisons must be treated with caution. Despite these limitations, a 2x4 factorial ANOVA was conducted to test for possible

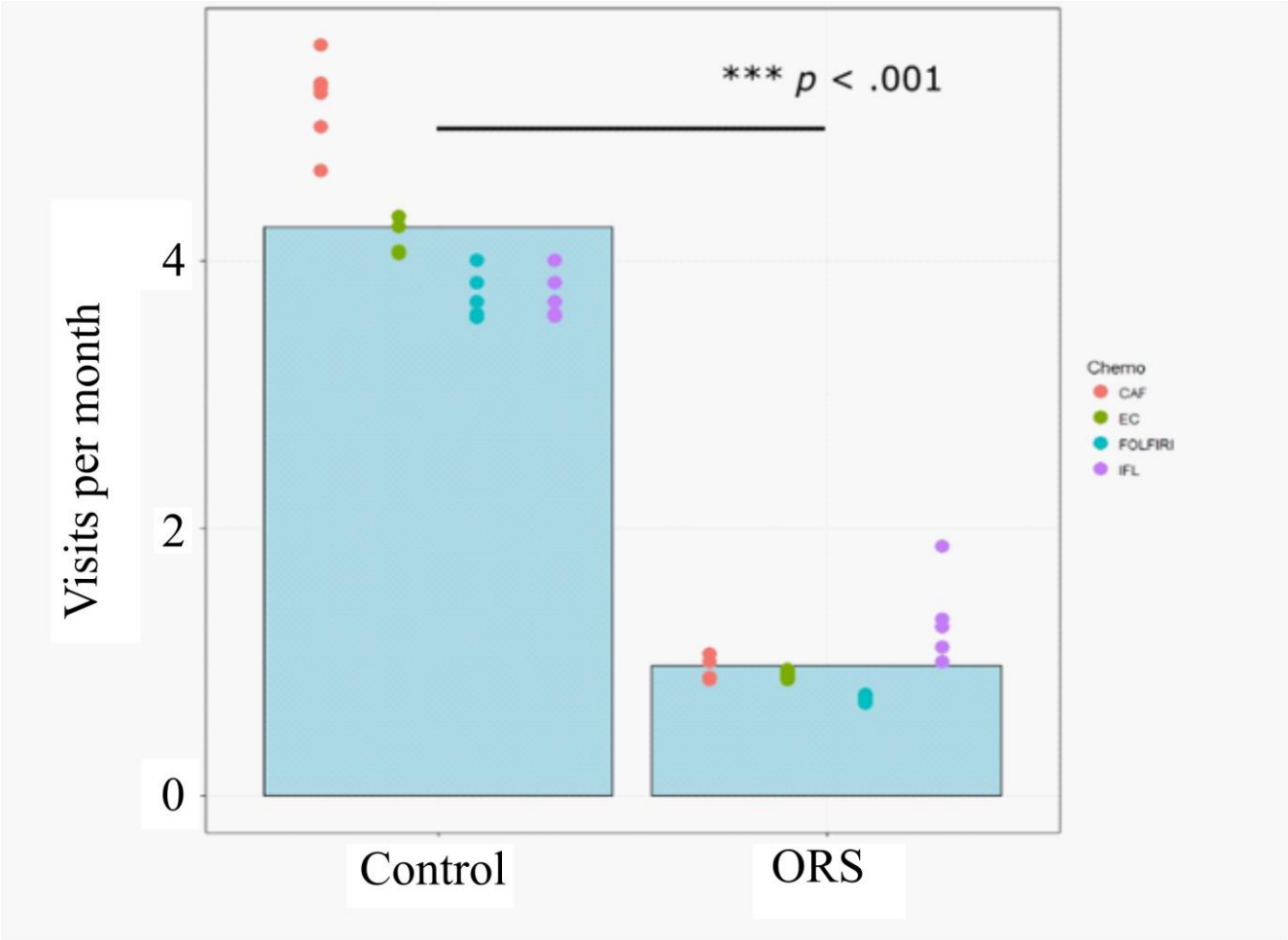

Figure 1: Patients who were given ORS had far fewer return visits than patients who were not.

City	Control CAF	EC	FOLFIRI	IFL	ORS CAF	EC	FOLFIRI	IFL
Baku	3				16			
Chonburi	6	14			24	36		
Gaborone	6			6	21			38
Gangtok	3				17			
Khartoum	4		5		14		52	
Lagos		6		8		45		28
Lampang			13	6			38	19
Lusaka		6		7		41		22
Lyon	7	14	10		31	48	56	
Nairobi		4	7			28	26	
Pulau Pinang			6	9			39	27
Total	29	44	41	36	123	198	211	134

Table 1: Patient counts per treatment per hospital.

City	Control CAF	EC	FOLFIRI	IFL	ORS CAF	EC	FOLFIRI	IFL
Baku	4.67				1			
Chonburi	5	4.07			0.88	0.94		
Gaborone	5.61			4.33	1			1.32
Gangtok	5.33				1.06			
Khartoum	5.25		4		0.86		0.75	
Lagos		4.5		4		0.86		1.11
Lampang			3.69	4			0.71	1.26
Lusaka		4.33		3.86		0.90		1
Lyon	5.29	4.07	3.6		1	0.92	0.70	
Nairobi		4.25	3.57			0.86	0.70	
Pulau Pinang			3.83	4.11			0.74	1.19
Mean	5.19	4.24	3.73	4.06	0.97	0.90	0.72	1.18

Table 2: Mean monthly visits per treatment per hospital.

differences between the chemotherapy treatments, or for interactions between treatment type and group.

Results:

By Group Comparisons

Mean monthly return rates per chemotherapy treatment type per hospital are given in Table 2. When treating the data from all the chemotherapy treatments as belonging to one factor: either the control or the ORS group, Levene's test found that the homogeneity of variance assumption was violated, $F(1,40) = 10.623$, $p = .002$. There was more variability for visit rates in the control group ($M = 4.35$, $SD = 0.61$) compared to visit rates in the ORS group ($M = 0.94$, $SD = 0.18$). This difference is likely attributable to the smaller sample size in the control group, which was kept small purposely so as to maximally reduce the suffering of patients in our study.

Welch's t was used to make our corrected group comparisons. It found a significant difference in monthly return visit rate between the control group and the ORS group, $t(23.386) = 24.5$, $p < .001$, $d = 7.58$. The effect size of this difference was remarkably large. Based on this comparison, it appears that supplying chemotherapy

patients with ORS significantly reduced their discomfort, and dramatically improved their health outcomes.

By Treatment Comparisons

When treating our data as belonging to multiple factors (Factor A being group; Factor B being chemotherapy treatment type) Levene's Test did not show a violation of the homogeneity of variance assumption at the alpha = .05 level, $F(7,34) = 1.63$, $p = .15$. Thus, a 2x4 factorial ANOVA was run without corrections. The to-be-expected main effect of the group on return visits per month $F(1, 34) = 2932.24$, $p < .001$, $\eta^2 = .92$ accounted for an overwhelming proportion of the variance. There was as well a main effect of treatment type, $F(3, 34) = 36.72$, $p < .001$, $\eta^2 = .03$ and an interaction effect of group and treatment type $F(3, 34) = 40.27$, $p < .001$ $\eta^2 = .04$. The general benefit of having ORS appears to heavily outweigh any differences between chemotherapy treatment types. As mentioned already, the low degrees of freedom provided by these data render comparisons of the treatment types unreliable, with an extremely low power of 1-ß = .22. As such, deeper analyses were not conducted. . Further research could elucidate whether there is a difference in the effectiveness for one chemotherapy treatment over another.

Discussion:

We studied a highly representative sample of patients undergoing one of several chemotherapy treatments from hospitals across almost a dozen countries. Patients who were given our low-osmolarity ORS had return visit rates that were less than 25% of those who were not. This study is the first to demonstrate such a large difference in the rehospitalization rates of chemotherapy patients as a direct result of ORS consumption.

It is worth mentioning that, prior to the official start of this study, in an unpublished pilot trial, we used an unflavored formulation of R^3. However, the native salty taste was unpalatable to most chemotherapy patients, and so they had difficulty consuming R^3 as instructed. We reformulated R^3 to include an organic, natural lemon flavoring to improve its palatability. Once the flavoring was added, patients no longer complained about the taste, and the clinical trials could be carried out properly.

The World Health Organization (WHO) concluded that a lower-osmolarity ORS formulation was needed to replace the previous hypo-osmolar formulation. This switch was motivated by improved medical outcomes, including reductions in stool output, vomiting, and the need for supplemental intravenous (IV) therapy (Binder et al., 2014; Duggan et al., 2004). The WHO lower-osmolarity ORS has an osmolarity of 245 mOsm/L. Our proprietary low-osmolarity formulation, R^3, has an even lower osmolarity of 172 mOsm/L. R^3 was highly successful in reducing hospital visit rates. It is possible that the WHO ORS could be successful to this end as well.

Cancer affects people of every socio-economic status, but results in higher mortality rates among lower HDI countries (Ferlay et al., 2015). These countries also have higher rates of mortality resulting from diarrhea (Santosham et al., 2010). ORS provide a cost-efficient treatment option, but budgetary, logistical, and bureaucratic concerns have made it difficult to improve the channels by which ORS are administered (Wilson et al., 2013; Isanka et al., 2012; Santosham et al., 2010; Walker, Fontaine, Young, & Black, 2009). Chemotherapy treatment may represent an avenue that can attract policy makers to improve access to ORS more generally.

Advances in hygiene, public awareness, and sanitation continue to reduce the infection and transmission rate of infectious diarrheal diseases (Jahan, 2016), and have lessened the prevalence of infection-related cancers in less developed countries. However, there have been simultaneous increases in cancers caused by dietary, hormonal, and reproductive factors (Bray, Jamal, Gray, Ferlay, & Forman, 2012). It is possible that the number of chemotherapy treatments will continue to increase. Our ORS formulation has been shown to help patients undergoing these treatments.

It is our hope that our findings will aid in motivating lawmakers to improve distribution channels for ORS, and encourage practitioners to consider using ORS to treat more diverse dehydrating maladies.

References:

Ang, C. W., Seretis, C., Wanigasooriya, K., Mahadik, Y., Singh, J., & Chapman, M. A. S. (2015). The most frequent cause of 90-day unplanned hospital

readmission following colorectal cancer resection is chemotherapy complications. *Colorectal Disease*, *17*(9), 779–786. https://doi.org/10.1111/codi.12945

Binder, H. J., Brown, I., Ramakrishna, B. S., & Young, G. P. (2014). Oral Rehydration Therapy in the Second Decade of the Twenty-first Century. *Current Gastroenterology Reports*, *16*(3). https://doi.org/10.1007/s11894-014-0376-2

Bray, F., Jemal, A., Grey, N., Ferlay, J., & Forman, D. (2012). Global cancer transitions according to the Human Development Index (2008–2030): a population-based study. *The Lancet Oncology*, *13*(8), 790–801. https://doi.org/10.1016/s1470-2045(12)70211-5

Daly, L. E., Bhuachalla, É. N., Cushen, S., Power, D., O'Reilly, S., McEneaney, P., ... & Ryan, A. (2016). Malnutrition in 822 Irish cancer patients undergoing chemotherapy: prevalence and impact on quality of life and survival. *Annals of Oncology*, *27*(suppl_6).

Duggan, C. (2004). Scientific Rationale for a Change in the Composition of Oral Rehydration Solution. *JAMA*, *291*(21), 2628. https://doi.org/10.1001/jama.291.21.2628

El-Sharkawy, A. M., Sahota, O., & Lobo, D. N. (2015). Acute and chronic effects of hydration status on health. *Nutrition Reviews*, *73*(suppl 2), 97–109. https://doi.org/10.1093/nutrit/nuv038

Ferlay, J., Shin, H.-R., Bray, F., Forman, D., Mathers, C., & Parkin, D. M. (2010). Estimates of worldwide burden of cancer in 2008: GLOBOCAN 2008. *International Journal of Cancer*, *127*(12), 2893–2917. https://doi.org/10.1002/ijc.25516

Ferlay, J., Soerjomataram, I., Dikshit, R., Eser, S., Mathers, C., Rebelo, M., … Bray, F. (2014). Cancer incidence and mortality worldwide: Sources, methods and major patterns in GLOBOCAN 2012. *International Journal of Cancer*, *136*(5), E359–E386. https://doi.org/10.1002/ijc.29210

Gill, C. J., Young, M., Schroder, K., Carvajal-Velez, L., McNabb, M., Aboubaker, S., … Bhutta, Z. A. (2013). Bottlenecks, barriers, and solutions: results from multicountry consultations focused on reduction of childhood pneumonia and diarrhoea deaths. *The Lancet*, *381*(9876), 1487–1498. https://doi.org/10.1016/s0140-6736(13)60314-1

Iro, M. A., Sell, T., Brown, N., & Maitland, K. (2018). Rapid intravenous rehydration of children with acute gastroenteritis and dehydration: a systematic review and meta-analysis. *BMC Pediatrics*, *18*(1). https://doi.org/10.1186/s12887-018-1006-1

Isanaka, S., Elder, G., Schaefer, M., Vasset, B., Baron, E., & Grais, R. (2012). Bridging the gap from knowledge to delivery in the control of childhood diarrhoea. *Bulletin of the World Health Organization*, *90*(9), 635–635. https://doi.org/10.2471/blt.12.109504

Jahan, S. (2016). Cholera – Epidemiology, Prevention and Control. Significance, Prevention and Control of Food Related Diseases. https://doi.org/10.5772/63358

Jaspers, L., Colpani, V., Chaker, L., van der Lee, S. J., Muka, T., Imo, D., … Franco, O. H. (2014). The global impact of non-communicable diseases on households and impoverishment: a systematic review. *European Journal of Epidemiology*, *30*(3), 163–188. https://doi.org/10.1007/s10654-014-9983-3

Jemal, A., Bray, F., Center, M. M., Ferlay, J., Ward, E., & Forman, D. (2011). Global cancer statistics. *CA: A Cancer Journal for Clinicians*, *61*(2), 69–90. https://doi.org/10.3322/caac.20107

Kelly, K. J., Cajas, L., Baumgartner, J. M., & Lowy, A. M. (2017). Factors Associated with 60-Day Readmission Following Cytoreduction and Hyperthermic Intraperitoneal Chemotherapy. *Annals of Surgical Oncology*, *25*(1), 91–97. https://doi.org/10.1245/s10434-017-6108-8

Kühn, J., Finger, F., Bertuzzo, E., Borgeaud, S., Gatto, M., Rinaldo, A., & Blokesch, M. (2014). Glucose- but Not Rice-Based Oral Rehydration Therapy Enhances the Production of Virulence Determinants in the Human Pathogen Vibrio cholerae. *PLoS Neglected Tropical Diseases*, *8*(12), e3347. https://doi.org/10.1371/journal.pntd.0003347

Martin, A. S., Abbott, D. E., Hanseman, D., Sussman, J. E., Kenkel, A., Greiwe, P., … Ahmad, S. A. (2016). Factors Associated with Readmission After Cytoreductive Surgery and Hyperthermic Intraperitoneal Chemotherapy for Peritoneal Carcinomatosis. *Annals of Surgical Oncology*,

23(6), 1941–1947. https://doi.org/10.1245/s10434-016-5109-3

Muchmore, J. H., & Wanebo, H. J. (2008). Regional Chemotherapy: Overview. *Surgical Oncology Clinics of North America*, *17*(4), 709–730. https://doi.org/10.1016/j.soc.2008.04.013

Okeke, I. N., Laxminarayan, R., Bhutta, Z. A., Duse, A. G., Jenkins, P., O'Brien, T. F., … Klugman, K. P. (2005). Antimicrobial resistance in developing countries. Part I: recent trends and current status. *The Lancet Infectious Diseases*, *5*(8), 481–493. https://doi.org/10.1016/s1473-3099(05)70189-4

Qadri, F., Svennerholm, A.-M., Faruque, A. S. G., & Sack, R. B. (2005). Enterotoxigenic Escherichia coli in Developing Countries: Epidemiology, Microbiology, Clinical Features, Treatment, and Prevention. *Clinical Microbiology Reviews*, *18*(3), 465–483. https://doi.org/10.1128/cmr.18.3.465-483.2005

Santosham, M., Chandran, A., Fitzwater, S., Fischer-Walker, C., Baqui, A. H., & Black, R. (2010). Progress and barriers for the control of diarrhoeal disease. *The Lancet*, *376*(9734), 63–67. https://doi.org/10.1016/s0140-6736(10)60356-x

Sinno, M. H., Coquerel, Q., Boukhettala, N., Coëffier, M., Gallas, S., Terashi, M., … Fetissov, S. O. (2010). Chemotherapy-induced anorexia is accompanied by activation of brain pathways signaling dehydration. *Physiology & Behavior*, *101*(5), 639–648. https://doi.org/10.1016/j.physbeh.2010.09.016

Sullivan, E. S., Ní Bhuachalla, E., Cushen, S., Power, D. G., Ryan, A. M., & Daly, L. (2018). Malnutrition and body composition predict poor quality of life and reduced survival in ambulatory oncology patients receiving chemotherapy: a cross sectional study of 1015 patients. *Proceedings of the Nutrition Society*, *77*(OCE1). https://doi.org/10.1017/s0029665117004244

Ververs, M., & Narra, R. (2017). Treating cholera in severely malnourished children in the Horn of Africa and Yemen. *The Lancet*, *390*(10106), 1945–1946. https://doi.org/10.1016/s0140-6736(17)32601-6

Fischer Walker, C. L., Fontaine, O., Young, M. W., & Black, R. E. (2009). Zinc and low osmolarity ORS for diarrhoea: a renewed call to action. *Bulletin of the World Health Organization*, *87*(10), 780–786. https://doi.org/10.2471/blt.08.058990

Wilson, S. E., Morris, S. S., Gilbert, S. S., Mosites, E., Hackleman, R., Weum, K. L. M., … Hawes, S. E. (2013). Scaling up access to oral rehydration solution for diarrhea: Learning from historical experience in low– and high–performing countries. *Journal of Global Health*, *3*(1). https://doi.org/10.7189/jogh.03.010404

Volume 1, Article 2; Pages 10-25 Doi: 10.31013/2001b

Measuring the bioactivity of phytocannabinoid cannabidiol from cannabis sources, and a novel non-cannabis source

D. Cushing[1]*, S. Kristipati[2], R. Shastri[2], & B. Joseph[1]

[1]: Peak Health Center, Los Gatos, CA
[2]: Endocrine BioTech, Newark, CA

*For inquiries, email corresponding author at donish@peakhealth.center

Recieved: March 18, 2018

Accepted: March 24, 2018

Published: April 2, 2018

Citation: Cushing, C., Kristipati, S., Shastri, R., & Joseph, B. (2018). Measuring the bioactivity of phytocannabinoid cannabidiol from cannabis sources, and a novel non-cannabis source. *Journal of Medical Phyto Research, 1*(2), 8-23. https://doi.org/10.31013/1002b

Abstract

Phytocannabinoid Cannabidiol (CBD) has been shown to elicit a great many immunological benefits. It acts on the endocannabinoid system, namely through interactions with cannabinoid receptor 2 (CB2). CBD-CB2 affinity, which we refer to as bioactivity, is rarely tested for clinical samples. We believe that uncontrolled variation in bioactivity levels have been silently confounding many CBD experiments. In our four-part study, we validate an efficient bioactivity test that can enable greater scientific control over CBD studies. We use it to compare the bioactivity of CBD obtained from different plant organs, and we also studied whether processing methods play a role in determining bioactivity. We also examine the bioactivity and processing factors of a novel non-cannabis plant capable of producing CBD in commercial quantities, named *Humulus Kriya* (*H. Kriya*, U.S. Patent No. 15/932,529, 2018). We also test the bioactivity of some CBD isolates/extracts currently sold in the market, and compare them with a CBD product called ImmunAG, which was extracted from the inflorescence of *H. Kriya*. We find that the CBD from the inflorescence of the plant produces the highest bioactivity, followed by the apical buds/leaves, the petioles, and finally the stalk. We find that *H. Kriya* has a bioactivity profile similar to *Cannabis Sativa*. We find that the bioactivity levels among cannabis-based commercial CBD products are quite low, and variable. We find significantly higher bioactivity levels in ImmunAG.

In recent years, there has been a great surge in scientific research involving the Phytocannabinoid Cannabidiol (CBD) (Burstein, 2015; Zuardi, 2008). CBD appears to have an acceptable, if not favorable safety profile (Iffland, & Grotenhermen, 2017; Devinsky et al., 2016) and has been shown to be anxiolytic, antidepressant,

antipsychotic, anticonvulsant, anti-nausea, antioxidant, anti-inflammatory, anti-arthritic, and anti-neoplastic (Ligresti, De Petrocellis, & Di Marzo, 2016). It has shown to be protective in animal models of epilepsy, anxiety, psychosis, and basal ganglia diseases (Ligresti, De Petrocellis, & Di Marzo, 2016). Anti-cancer effects have also been shown (Pisanti et al., 2017).

Of the receptors upon which CBD acts, cannabinoid receptor 2 (CB_2) has the most ubiquitous, well-studied presence in the immune system (Malfitano, Basu, Maresz, Bifulco, & Dittel, 2014). CB_2 presents in NK cells, B cells, monocytes, CD4+ cells, CD8+ cells, T cells, and neutrophils (Malfitano, Basu, Maresz, Bifulco, & Dittel, 2014; Tanasescu, Gran, & Constantinescu, 2013; Pacher & Mechoulam, 2011), and it appears to be the key mediator for cannabinoid regulation of inflammation and other immune functions (Ashton & Glass, 2007; Xiong et al., 2012; Lunn et al., 2006; McKallip et al., 2002; McKallip, Lombard, Martin, & Nagarkatti, 2002).

We refer to the affinity for CBD to interact with CB_2 as its bioactivity[1,2]. Historically, CBD bioactivity tests have relied on costly and short-lived biological tools (e.g., transfected CHO membranes). Experiments in which the bioactivity of a CBD sample was tested, and subsequently used in clinical trials, have been prohibitively expensive and time consuming to carry out. We believe that uncontrolled variation in bioactivity levels have been silently confounding many CBD experiments.

The factors underlying variability in CBD bioactivity have never been publicly identified. Possible candidates include organ source within the plant, and the extraction/processing methodology. These factors vary wildly among suppliers. Many legalities surrounding *Cannabis Sativa*, the plant from which CBD has traditionally been extracted, reinforce idiomatic peculiarities. In the United States, despite a federal ban on all cannabis-based CBD extractions (Mead, 2017), some state governments have unique laws sanctioning the supply of cannabis-based CBD products (Cambron, Guttmannova, & Fleming, 2017). State-funded research utilizes cannabis plants with different cannabinoid profiles than what is grown and used in the legal market (Vergara et al., 2017). Research that is funded by, independently run, private organizations, in the commercial sector often utilize their own CBD isolates/extracts (e.g., French et al., 2017). Taken together, laws, regulations, and practices reinforce the problem of variability in CBD bioactivity.

In the present article, we validate a more efficient bioactivity test that can enable greater scientific control over CBD studies. We explore two factors responsible for cannabis-based CBD bioactivity: the plant organ source from which the CBD is extracted, and the extraction method. We also examine the bioactivity, per organ, and extraction method of a novel, proprietary, non-cannabis plant capable of producing CBD in commercial quantities, named *Humulus Kriya* (*H. Kriya*, U.S. Patent No. 15/932,529, 2018). We then test the bioactivity of some CBD isolates/extracts currently sold in the market, and compare them with CBD extracted from *H. Kriya* with knowingly controlled bioactivity factors.

Experiment 1: A novel, valid, scalable CBD bioactivity test

[1] Bioactivity refers to the intensity of the biological response that results when a ligand makes contact with its intended target. Generally, a more bioactive ligand causes a more pronounced effect. Bioactivity should not be confused with bioavailability, which is the rate of diffusion of a substance through membranes to reach the intended target in the body.

[2] CBD displays potent antagonism of CB2 receptor agonists (Pertwee, 2008; Thomas et al., 2007) and has also been shown to function as an inverse agonist at CB_2 (Pertwee, 2008; Pertwee et al., 2010). CBD acts as an antagonist preventing [35S]GTPγS binding and Rho activation (Ryberg et al., 2007; Whyte et al., 2009; Ford et al., 2010), modulating Ca2+ mobilization (Lauckner et al., 2008) and β-arrestin recruitment (Yin et al., 2009). CB2 inverse agonism can block migration of immune cells and decrease inflammation (Lunn et al., 2006). CBD potently inhibits migration of macrophages, microglial cells and neutrophils (Walter et al., 2003; Sacerdote et al., 2005). CBD-induced block of chemotaxis of macrophages can be prevented by SR144528, a CB2 selective antagonist (Sacerdote et al., 2005). CBD potently inhibits forskolin-stimulated cyclic AMP production by human CB2 receptor-expressing CHO cells (Gauson, Stevenson, Thomas, Baillie, Ross, & Pertwee, 2007).

Highly pure, naturally occurring CBD molecules were extracted from the *Avidekel* plant, obtained in 2014 from Tikun Olam, Israel, via sonic fractionation and ultra centrifugal separation.

[3h]-CP55940 displacement assays were performed for this reference sample using membrane fractions of CHO cells expressing recombinant human CB_2. Additionally, binding of an MCA (described in U.S. Patent No. 62,599,501, 2017) was tested for this

reference sample. The resulting displacement and binding values were used as a reference standard

against which 26 CBD samples (acquired from Natural Hemp Solutions, Atlanta Georgia) were compared.

We looked for a correlation between the CHO CB_2 binding, and the MCA binding across 26 samples. If the MCA binding correlated to the CHO-CB_2, it could be used instead for quicker, more efficient testing.

Results:

Pearson correlation analysis was performed using R on the CB_2 and CAC binding values of the 26 CBD samples. The binding affinities to both the recombinant human CB_2 and the highest-affinity MCA are listed in Table 1 as a proportion relative to the binding affinity shown by a highly pure CBD molecule. Using the Pearson correlation analysis, we found that these were highly correlated (Pearson coefficient = .97). Thus, we can predict the bioactivity of CBD using the MCA with high accuracy.

Discussion:

We have validated a successful and scalable bioactivity test for CBD. Bioactivity values are expressed as a proportion between 0 and 1 as compared to the CHO-CB_2 binding of the purest CBD molecule we could isolate. The lower the number, the lower the bioactivity. If a CBD molecule has a bioactivity below 0.5, one could expect to observe CBD-CB2 binding at half the strength of a molecule with a bioactivity of 1. If a molecule had an observed bioactivity of 0.2, one could expect the binding affinity to be at 1/5 the strength of a molecule with a bioactivity of 1. This test will illuminate the distribution of bioactive molecules throughout various parts of the plant.

Sample	MCA Affinity	CB2 Affinity
1	0.78	0.81
2	0.34	0.42
3	0.25	0.29
4	0.32	0.3
5	0.34	0.36
6	0.31	0.33
7	0.24	0.25
8	0.29	0.34
9	0.32	0.3
10	0.29	0.31
11	0.25	0.25
12	0.31	0.32
13	0.35	0.33
14	0.31	0.31
15	0.25	0.26
16	0.3	0.31
17	0.27	0.24
18	0.25	0.24
19	0.32	0.29
20	0.21	0.24
21	0.26	0.24
22	0.44	0.41
23	0.33	0.41
24	0.81	0.8
25	0.3	0.22
26	0.19	0.22
27	0.78	0.81
28	0.34	0.42

Table 1: Binding affinities for the MCA versus the CB2 complex in 26 CBD-producing plant samples. They were highly correlated (r = .97).

Experiment 2: Cannabis CBD bioactivity by plant organ

It is well known, among growers, that the yield of CBD is variable across different organs in the cannabis plant, with the inflorescence producing the highest output[3]. (We have replicated this in a to-be-published study.) However, the bioactivity of CBD extracted from different organs has never been studied before.

Using the bioactivity test, validated in experiment 1, we examined 4 regions from 48 different cultivars of cannabis obtained from the USA, India, China, and the Czech Republic. Inflorescence, petioles, apical buds/leaves, and stalks were tested separately. A combination of sonic fractionation and ultra centrifugal separation was used on the inflorescence to obtain purified samples. We also used cold solvent extraction to obtain CBD from the inflorescence, petioles, apical buds/leaves, and stalks.

Results:

A 1x5 ANOVA and appropriate post-hoc comparisons were conducted on bioactivity with plant organ as the only factor. Bioactivity means and standard errors were plotted.

Levene's test indicated heteroscedastic variances between the organs $F(4,235) = 6.05$, $p < .001$. As such, we conducted a robust ANOVA as described by Wilcox (2012). It found a significant difference between the bioactivities of centrifuge-extracted inflorescence CBD ($M = .96$, $SD = .02$, solvent-extracted CBD from the inflorescence ($M = .86$, $SD = .04$), solvent-extracted CBD from the petioles ($M = .54$, $SD = .03$), solvent-extracted CBD from the apical buds/leaves ($M = .4$, $SD = .04$), and solvent-extracted CBD from the stalks ($M = .19$, $SD = .02$), $F(4, 70.38) = 9885.21$, $p < .001$. (20% trimmed means are presented above.)

Robust post-hoc comparisons (Mair & Wilcox, 2016), revealed significant differences between each of the CBD source categories. (See Table 2 for the psihat values of each comparison, and their associated confidence intervals.) In summary, the highest bioactivity CBD was

	Inflorescence	Petioles	Apical Buds/Leaves	Stalks
Inflorescence Centrifuge	-.205 [-.222 to -.187]	-.769 [-.781 to -.756]	-.669 [-.685 to -.654]	-.344 [-.360 to -.329]
Inflorescence		-.563 [-.583 to -.545]	-.464 [-.486 to -.443]	-.140 [-.161 to -.119]
Petioles			.099 [.082 to .117]	.424 [.407 to .441]
Apical buds/Leaves				.325 [.305 to .344]

Table 2. Psihat and corresponding confidence interval values (in brackets) for robust one-way ANOVA post-hoc comparisons of bioactivity. Psihat values for each post-hoc comparions were obtained using 20% trimmed means. Corresponding 95% confidence interval values are presented in brackets. All associated *p*-values were < .001.

[3] The tip of secreting hairs located mainly on female-plant contain resin glands that have a considerable amount of cannabinoids. These glands are fewer in number in the leaves (Zuardi, 2008).

found in the pods of each plant, with decreasing bioactivity in the petioles, apical buds/leaves, and stalks respectively (See Figure 1). (Individual bioactivity scores obtained per plant are provided in Appendix 1.)

Discussion

Our results showed a difference between extraction methodologies. The combination of sonic fractionation and ultra centrifugal separation produced CBD with the highest bioactivity. Sonic fractionation and ultra centrifugal extraction are labor- and equipment-intensive laboratory procedures, not fit for large-scale manufacture. By contrast, ethanol solvent extraction causes a small amount of degradation in bioactivity, but is scalable and relatively

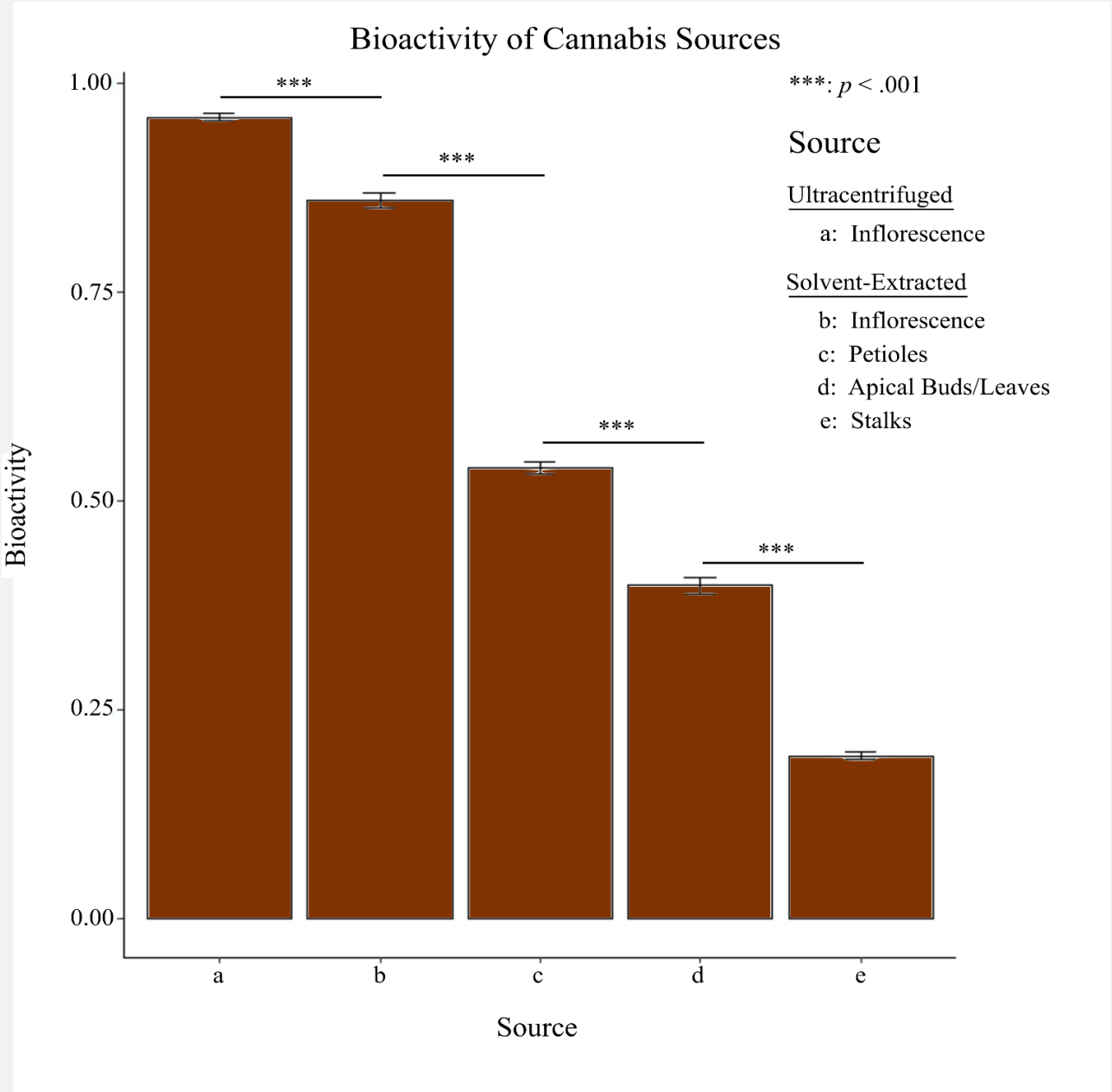

Figure 1: A highly canonical pattern emerged with inflorescence producing the highest bioactivity. CBD source a was obtained through ultra centrifugal separation. CBD sources b, c, d, and e were obtained through cold-solvent ethanol extraction. Standard errors shown above are from untrimmed means to show the most statistically conservative estimates.

inexpensive to carry out. Ergo, it is a far more common procedure for commercial CBD production[4].

Among plant organs subjected to ethanol extraction, our results indicate a canonical pattern of CBD bioactivity. The inflorescence produced the highest bioactivity CBD molecules, with levels five times higher than CBD extracted from the stalk. Inflorescence should be used exclusively for the production of high bioactivity CBD. If commercial CBD suppliers have mixed in biomass from the stem and bark of the plant before extraction, it has lily led to low bioactivity in their products.

Experiment 3: Testing the bioactivity of a novel, non-cannabis, plant source of CBD

Using a plant from the Humulus family that produces CBD, a new plant was developed called *Humulus Kriya*. It does not produce THC, is from a family of plants considered GRAS (FDA Title 21, Volume 3, Sec 182.2-CAS 8060-28-4) and has been certified by FSSAI (Food Safety and Standards Authority of India) as a "Food Ingredient". It should not fall under the Scheduled List classification. We tested the bioactivity profile of the various parts of *H. Kriya* using the same methods as in experiment 2.

[4] It is worth noting that many other extraction processes exist (e.g., CO_2 and freon extraction). Inflorescence should produce the most bioactive CBD regardless of extraction methodology but further research needs to be done to confirm this.

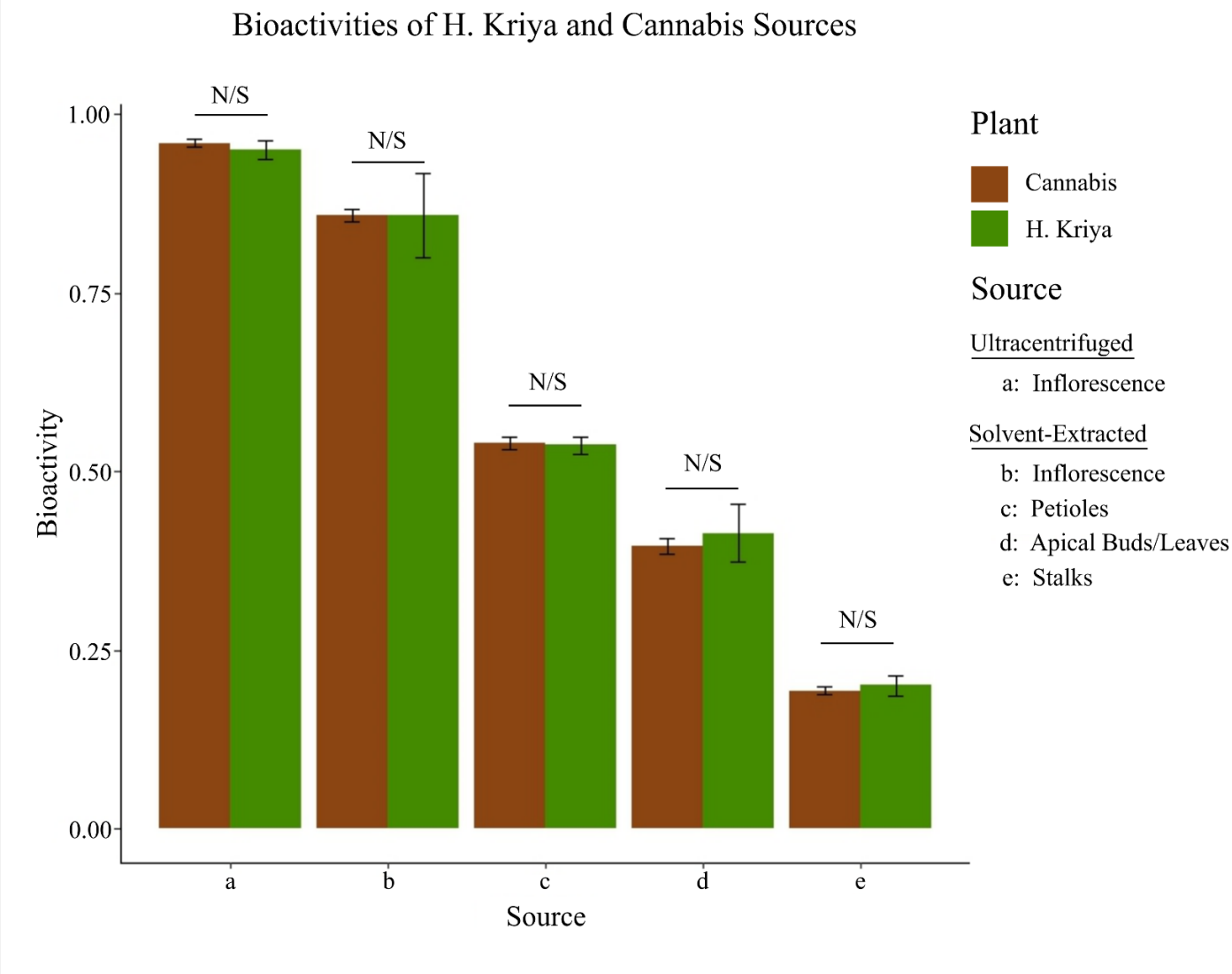

Figure 2: No significant differences were found between *H. Kriya* and cannabis for any of the organs.

Results: Our samples were made of Six *H. Kriya* plants, provided by ImmunAG, LLP, India, and thirty one samples of ImmunAG oil extract.

We used Welch's *t* to compare CBD bioactivity of *H. Kriya* from all five groups to the cannabis samples (Comparisons are shown in Figure 2. Individual bioactivity scores obtained per plant are provided in Appendix 2.) The centrifuged pod CBD from *H. Kriya* (M = .95, SD = .01) showed no difference in bioactivity compared to cannabis samples, $t(8.6594) = 1.74$, $p = .12$. The solvent extracted pod CBD (M = .86, SD = .06) showed no difference, $t(5.3803) = 0.007$, $p = .99$. The solvent-extracted petiole CBD (M = .54, SD = .01) showed no difference, $t(14.123) = 0.373$, $p = .715$. The solvent-extracted leaf CBD (M = .41, SD = .04) showed no difference, $t(6.164) = -1.0212$, $p = .346$. The solvent-extracted stem CBD (M = .20, SD = .01) showed no difference, $t(7.322) = -1.143$, $p = .289$. It appears as though *H. Kriya* has an identical CBD bioactivity profile to the cannabis strains we tested.

Discussion:

We found identical CBD bioactivity between *H. Kriya* and Cannabis for CBD extracted from various parts of the plant. *H. Kriya* appears to be a viable cannabis alternative for CBD research. CBD from *H. Kriya* has no risk of THC contamination. It has been certified as a food ingredient by the Food Safety and Standards Authority of India.

Experiment 4: Examining the Bioactivity of commercially available CBD products

The bioactivity of commercial CBD samples has never been examined. We are publishing results of commercial, cannabis-based, products analyzed over the past 2 years. These samples were sent to us directly by vendors (Natural Hemp Solutions, Centuria Foods, BSPG, Isodiol, Hammer Enterprises, etc.) or sent to us by 3rd parties. We have deliberately not published the bioactivity results for individual vendors and have anonymously presented the bioactivity results for all of the vendors together.

There are many cannabimimetic molecules other than CBD. The two announced sources of CBD from non-hemp/cannabis sources are yeast and humulus. We attempted for a while but could not get samples of CBD extracted from yeast. We tested the bioactivity of CBD extracted from *H. Kriya* (ImmunAG), and compared it to commercial cannabis products.

Results:

The minimum bioactivity in commercial samples was 0.11 and the maximum was 0.41. The minimum bioactivity in ImmunAG was 0.72, and the maximum was 0.98. Bioactivity scores for both classes of product are shown in Figure 3.

When comparing the CBD bioactivity in ImmunAG (*M* = .88, *SD* = .06) to products on the market

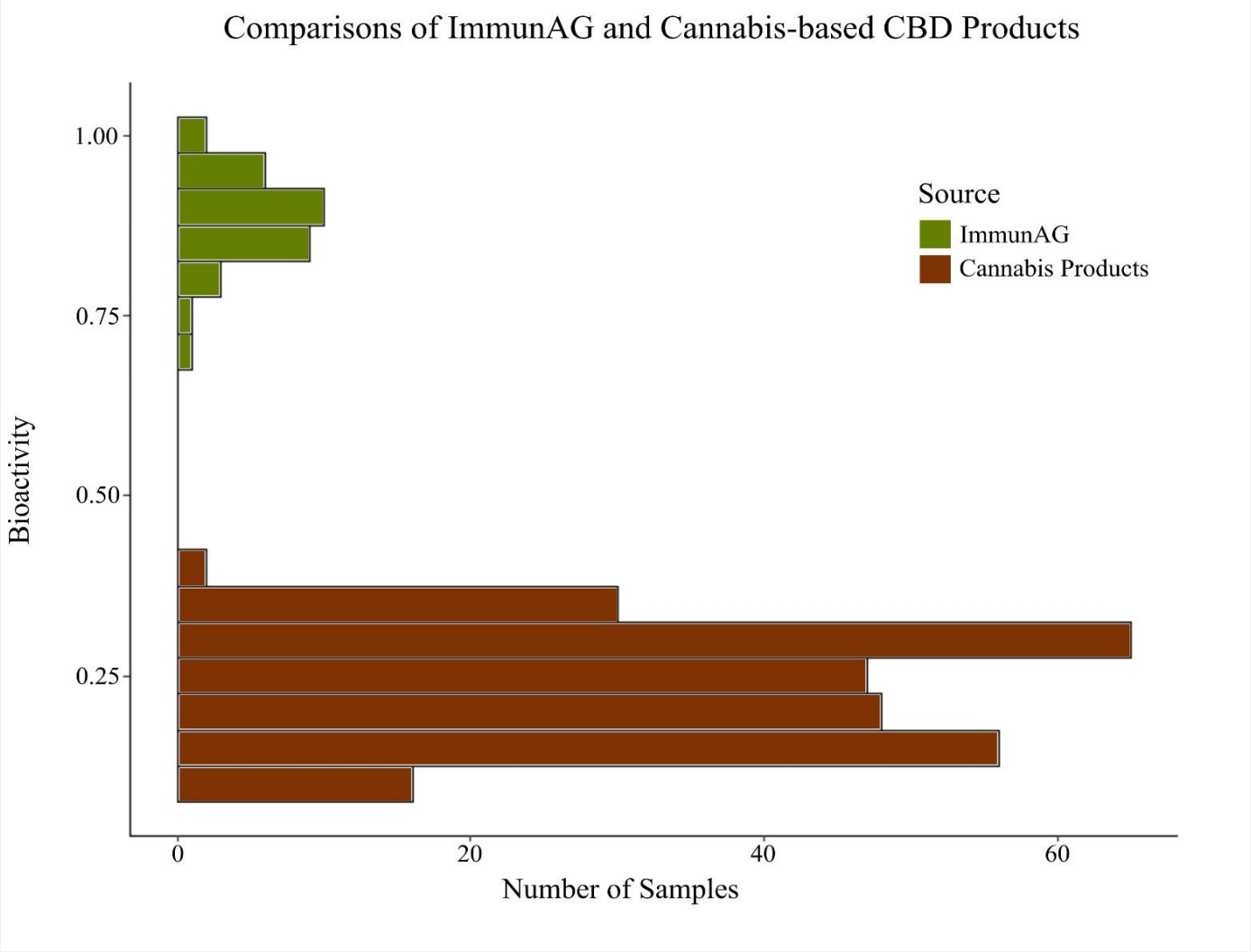

Figure 3: *H. Kriya*-based ImmunAG shows higher bioactivity across all samples than cannabis-based commercial products.

(M = .23, SD = .07), Welch's t found a significant difference in bioactivity, $t(41.288) = 53.41$, $p < .001$.

Discussion:

Commercial CBD bioactivity were low, having values consistent with the lower bioactive organs— stalks, stems, barks and leaves. It is possible that suppliers have been using biomass rich in stalk, stem and leaves to comply with regulations and increase mass. The caution is that low bioactive CBD may not produce desirably intense immunologic cell signals. Commercial CBD bioactivity were also quite variable, with a minimum of 0.11 and a maximum of 0.41. The highest commercial sample had almost four times the potency of the lowest sample. Left unchecked, low bioactivity CBD are likely to confound medical use or research and produce spurious results.

ImmunAG samples ranged from 0.72 to 0.98, with the lowest ImmunAG bioactivity higher than the highest commercial cannabis-based CBD bioactivity. This is not surprising because ImmunAG is only made from the inflorescence of *H. Kriya*. An audit revealed that carefully regulated processing conditions also enabled ImmunAG to maintain significantly high bioactivity. The effects of processing conditions on CBD bioactivity will be published in a subsequent paper.

Conclusions:

We found that use of mono clonal antibody testing of CBD bioactivity was viable. We found that CBD extracted from different plant organs had different bioactivity, with inflorescence having the highest bioactivity, and stalks/stems having the lowest. We evaluated a non cannabis CBD-producing plant, *H. Kriya*, that has a bioactivity profile similar to cannabis. We found that hemp/cannabis based CBD products sold commercially have low bioactivity. We found that commercial CBD products made from it *H. Kriya* had the highest bioactivity.

CBD-CB2 interactions are responsible for a wide range of immunologic effects. The samples we studied had widely varying levels of bioactivity. We believe it is likely that bioactivity levels have been silently confounding historical research results. Scientific studies utilizing CBD for medical research should strive to use products with the highest bioactivity levels.

Method:

CHO cells and membrane preparation

These were stably transfected with cDNA encoding human CB2 receptors. The CB_2-transfected cells used in binding assays with [$_3$H]-CP55940, [$_3$H]-WIN55212-2 or [$_{35}$S]-GTPγS (Bmax=72.5 pmol mg−1 protein). The clones used in the assays were the same as those used in the sPAP reporter assay described by Green *et al.* (1998). Cells were maintained at 37°C and 5% CO2 in DMEM (f-12 HAM) with 2 mm Glutamine, Geneticin (600 μg ml−1) and Hygromycin (300 μg ml−1). Because receptor over expression may lead to the activation of effector mechanisms to which receptors in natural membranes are not normally coupled (see Kenakin, 1995), the assays were performed with cells expressing fewer CB_2 receptors than the cells used in the binding assays.

CHO cells were suspended in 50 mm Tris buffer (pH 7.4) and 0.32 m sucrose and homogenized with an Ultra-Turrex homogenizer. The homogenate was diluted with 50 mm Tris buffer (pH 7.4) and centrifuged at 50,000×*g* for 1 h to isolate the membranes.

CHO-CB_2 binding

A filtration procedure was used to measure [$_3$H]-CP55940 and [$_3$H]-WIN55212-2 binding. This is a modification of the method described by Compton *et al*. (1993). Binding assays were performed with [$_3$H]-CP55940 or [$_3$H]-WIN55212-2, 1 mm MgCl2, 1 mm EDTA, 2 mg ml−1 bovine serum albumin (BSA) and 50 mm Tris buffer, total assay volume 500 μl. Binding was initiated by the addition of cell membranes (20–30 μg protein). Assays were carried out at 30°C for 90 min before termination by addition of ice-cold wash buffer (50 mm Tris buffer, 1 mg ml−1 BSA) and vacuum filtration using a 12-well sampling manifold (Brandel Cell Harvester) and Whatman GF/B glass-fibre filters that had been soaked in wash buffer at 4°C for 24 h. Each reaction tube was washed three times with a 4 ml aliquot of buffer. The filters were oven-dried for 60 min and then placed in 5 ml of scintillation fluid (Ultima Gold XR, Packard). Radioactivity was quantified by liquid scintillation spectrometry. Specific binding was defined as the difference between the binding that occurred in the presence and absence of 1 μm reference cannabidiol. Protein assays were performed using a Bio-Rad Dc kit. Unlabeled and radio labelled cannabidiol were each added in a volume of 50 μl following dilution in assay buffer (50 mm Tris buffer containing 10 mg ml−1 BSA). The concentration of [$_3$H]-CP55940 or [$_3$H]-WIN55212-2 used in displacement assays was 0.5 nm. The concentrations of cannabidiol that produced a 50% displacement of radio ligand from specific binding sites (IC50 values) were calculated using GraphPad Prism (GraphPad Software, San Diego, U.S.A.). Competitive binding curves were fitted

Labelled cannabinoid	Unlabelled cannabinoid	CB2 K_i (nM)
[^{3}H]-CP55940	CP55940	1.8±0.2
	L759633	6.4±2.2
	L759656	11.8±2.5
	AM630	31.2±12.4
	SR144528	5.6±1.1
[^{3}H]-WIN55212-2	AM630	37.5±15.4
	SR144528	4.1±1.3

Table 3: K_i values were calculated by the Cheng & Prusoff equation (n = 3 or 4) using K_D values of 0.8 nm for [^{3}H]-CP55940 in membranes of CB2 cells and a Kd value of 2.1 nm for [^{3}H]-WIN55212-2 in membranes of CB2 cells (Ross & Pertwee, unpublished).

with minimum values for displacement of radio ligand from specific binding sites constrained to zero. Dissociation constant (*K*i) values were calculated using the equation of Cheng & Prusoff (1973) and dissociation constant values of [$_3$H]-CP55940 and [$_3$H]-WIN55212-2 shown in the footnote to Table 3.

Generation and binding of the anti-CBD antibody

Reference CBD was extracted from the inflorescence of the *Avidekel* plant. 5% reference CBD was dissolved in caproic acid ($C_5H_{11}COOH$). 0.2 ml of this solution was injected with a 27-28 mm gage needle into the lateral tail vein of BALB/Lac mice. The injections were repeated every other day for 14 days for a total of 7 injections. Each injection was followed by an *in vivo* electroporation of 80 pulses of 100 microseconds at 0.3 Hz with an electrical field magnitude of 2500 V/cm. Following cannabidiol immunization, mouse splenocytes were extracted and isolated. They were fused with myeloma cells by dielectrophoresis using a BTX ECM 2001 Electrofusion Generator, manufactured by BTX Harvard Apparatus, Holliston, MA, USA. The fused cells were incubated in a hypoxanthine-aminopterin-thymidine medium (with respective concentrations 0.1 mM, 0.4 μM, and 0.016 mM) for between ten and fourteen days, resulting in the survival of only the B cell-myeloma hybrids. Following limiting dilution to one cell per plate, ELISA was used to select hybridomas that produced antibodies with higher binding to our pure CBD molecule. The antibody was linked to a Cytochrome P450 enzyme. We used Pentalenolactone as our Cytochrome P450 substrate. The hybridoma producing the antibody with the highest binding affinity, as measured by a molar weight increase in the Cannabidiol Antibody Complex (CAC), was cloned using supplemental media cultures containing interleukin-6. These procedures are additionally described in patent X.

Cloned hybridomas grew in culture medium RPMI-1640 with antibiotics and fetal bovine serum. A/G purification was used to extract monoclonal antibodies from hybridomas. The culture supernatant contained 46 micrograms/milliliter to 72 micrograms/milliliter of Cannabidiol monoclonal antibody (MCA). This antibody was maintained at -20ºC or lower until used. Fluorescence labelled ELISA was used to measure binding for each sample. The molar weight of the CAC was divided by the molar weight of the gold standard reference CAC to derive binding affinity values.

Ultracentrifugal CBD extraction:

Plant tissue (from the inflorescence) was ultrasonically fractioned. The pulp and plasma were separated by centrifugation. The plasma fraction was further fractionated and studied by analytical ultra centrifuge to obtain the sedimentation coefficient of CBD. Isopycnic density gradient preparative ultracentrifugation (up to 130,000 RPM), using sodium bromide and cesium chloride, was then done to collect the purified CBD

samples. This is not a commercially viable process but it provided enough mg of CBD to conduct the bioactivity test.

Solvent CBD extraction:

For the solvent procedure, we extracted dried plant material at around 20ºC with ethanol, followed by methylene chloride, and separated uncarboxylated cannabinoids from carboxylated cannabinoids.

CBD isolation and analysis:

Each fraction was identified by using the following methods: Silica gel eluting with $CHCl_3$; silica gel eluting with C_6H_6-MeOH-AcOH (88%: I 0%: 2%) (as in Mechoulam, Ben-Zvi, Yagnitinsky, & Shani, 1969); Korte and Sieper's (1964) published method; Cannabinoid reference standards.

Following CBD isolation and identification, Fast Blue B Salt colors were used for qualitative analysis. The cannabinoids were then analyzed after trimethyl-sililation, by GLC using OV225 (50' SCOT column) or OV17 (2% on Chromosorb W, 5' column). Acid cannabinoids were estimated after decarboxylation by heating in pyridine. Fluorescence labelled ELISA was used to measure the bioactivity of samples.

References:

Ashton, J. C., & Glass, M. (2007). The cannabinoid CB2 receptor as a target for inflammation-dependent neurodegeneration. *Current neuropharmacology*, *5*(2), 73-80. https://doi.org/10.2174/157015907780866884

Burstein, S. (2015). Cannabidiol (CBD) and its analogs: a review of their effects on inflammation. *Bioorganic & medicinal chemistry*, *23*(7), 1377-1385. https://doi.org/10.1016/j.bmc.2015.01.059

Cambron, C., Guttmannova, K., & Fleming, C. B. (2017). State and national contexts in evaluating cannabis laws: a case study of Washington state. *Journal of drug issues*, *47*(1), 74-90. https://doi.org/10.1177/0022042616678607

Compton, D. R., Rice, K. C., De Costa, B. R., Razdan, R. K., Melvin, L. S., Johnson, M. R., & Martin, B. R. (1993). Cannabinoid structure-activity relationships: correlation of receptor binding and in vivo activities. *Journal of Pharmacology and Experimental Therapeutics*, *265*(1), 218-226.

Devinsky, O., Marsh, E., Friedman, D., Thiele, E., Laux, L., Sullivan, J., ... & Wong, M. (2016). Cannabidiol in patients with treatment-resistant epilepsy: an open-label interventional trial. *The Lancet Neurology*, *15*(3), 270-278. https://doi.org/10.1016/s1474-4422(15)00379-8

Ford, L. A., Roelofs, A. J., Anavi-Goffer, S., Mowat, L., Simpson, D. G., Irving, A. J., ... & Ross, R. A. (2010). A role for L-α-lysophosphatidylinositol and GPR55 in the modulation of migration, orientation and polarization of human breast cancer cells. *British journal of pharmacology*, *160*(3), 762-771. https://doi.org/10.1111/j.1476-5381.2010.00743.x

French, J., Thiele, E., Mazurkiewicz-Beldzinska, M., Benbadis, S., Marsh, E., Joshi, C., ... & Sommerville, K. (2017). Cannabidiol (CBD) significantly reduces drop seizure frequency in Lennox-Gastaut syndrome (LGS): results of a multi-center, randomized, double-blind, placebo controlled trial (GWPCARE4)(S21. 001). *Neurology*, *88*(16 Supplement), S21-001.

Gauson, L. A., Stevenson, L. A., Thomas, A., Baillie, G. L., Ross, R. A., & Pertwee, R. G. (2007, June). Cannabigerol behaves as a partial agonist at both CB1 and CB2 receptors. In *Proceedings 17th Annual Symposium on the Cannabinoids. International Cannabinoid Research Society: Saint-Sauveur, QC* (p. 206).

Iffland, K., & Grotenhermen, F. (2017). An Update on Safety and Side Effects of Cannabidiol: A Review of Clinical Data and Relevant Animal Studies. *Cannabis and cannabinoid research*, *2*(1), 139-154. https://doi.org/10.1089/can.2016.0034

Joseph, B. (2018). *U.s. Patent No. 15/932,529.* Washington, DC: U.S. Patent and Trademark Office

Joseph, B. (2017). *U.S. Patent No. 62,599,501*. Washington, DC: U.S. Patent and Trademark Office.

Kenakin, T. (1995). Agonist-receptor efficacy II: agonist trafficking of receptor signals. *Trends in pharmacological sciences*, *16*(7), 232-238. https://doi.org/10.1016/s0165-6147(00)89032-x

Korte, F., & Sieper, H. (1964). Chemical classification of plants. XXIV. Hashish constituents by thin-layer chromatography. *Journal of Chromatography*, *13*(1), 90-98.

Lauckner, J. E., Jensen, J. B., Chen, H. Y., Lu, H. C., Hille, B., & Mackie, K. (2008). GPR55 is a cannabinoid receptor that increases intracellular calcium and inhibits M current. *Proceedings of the National Academy of Sciences*, *105*(7), 2699-2704. https://doi.org/10.1073/pnas.0711278105

Ligresti, A., De Petrocellis, L., & Di Marzo, V. (2016). From phytocannabinoids to cannabinoid receptors and endocannabinoids: pleiotropic physiological and pathological roles through complex pharmacology. *Physiological reviews*, *96*(4), 1593-1659. https://doi.org/10.1152/physrev.00002.2016

Lunn, C. A., Fine, J. S., Rojas-Triana, A., Jackson, J. V., Fan, X., Kung, T. T., ... & Narula, S. K. (2006). A novel cannabinoid peripheral cannabinoid receptor-selective inverse agonist blocks leukocyte recruitment in vivo. *Journal of Pharmacology and Experimental Therapeutics*, *316*(2), 780-788. https://doi.org/10.1124/jpet.105.093500

Mair, P., & Wilcox, R. (2016). *Robust Statistical Methods in R Using the WRS2 Package*. Technical report, Harvard University.

Malfitano, A. M., Basu, S., Maresz, K., Bifulco, M., & Dittel, B. N. (2014, October). What we know and do not know about the cannabinoid receptor 2 (CB2). In *Seminars in immunology* (Vol. 26, No. 5, pp. 369-379). Academic Press. https://10.1016/j.smim.2014.04.002

McKallip, R. J., Lombard, C., Fisher, M., Martin, B. R., Ryu, S., Grant, S., ... & Nagarkatti, M. (2002). Targeting CB2 cannabinoid receptors as a novel therapy to treat malignant lymphoblastic disease. *Blood*, *100*(2), 627-634. https://doi.org/10.1182/blood-2002-01-0098

McKallip, R. J., Lombard, C., Martin, B. R., Nagarkatti, M., & Nagarkatti, P. S. (2002). Δ9-Tetrahydrocannabinol-induced apoptosis in the thymus and spleen as a mechanism of immunosuppression in vitro and in vivo. *Journal of Pharmacology and Experimental Therapeutics*, *302*(2), 451-465. https://doi.org/10.1124/jpet.102.033506

Mead, A. (2017). The legal status of cannabis (marijuana) and cannabidiol (CBD) under US law. *Epilepsy & Behavior*, *70*, 288-291. https://doi.org/10.1016/j.yebeh.2016.11.021

Mechoulam, R., Ben-Zvi, Z., Yagnitinsky, B., & Shani, A. (1969). A new tetrahydrocannabinolic acid. *Tetrahedron letters*, *10*(28), 2339-2341. https://doi.org/10.1016/s0040-4039(01)88158-2

Pacher, P., & Mechoulam, R. (2011). Is lipid signaling through cannabinoid 2 receptors part of a protective system?. *Progress in lipid research*, *50*(2), 193-211. https://doi.org/10.1016/j.plipres.2011.01.001

Pertwee, R. G. (2004). The Pharmacology and Therapeutic. *Cannabinoids*, 32.

Pertwee, R. G. (2008). The diverse CB1 and CB2 receptor pharmacology of three plant cannabinoids: Δ9-tetrahydrocannabinol, cannabidiol and Δ9-tetrahydrocannabivarin. *British journal of pharmacology*, *153*(2), 199-215. https://doi.org/10.1038/sj.bjp.0707442

Pertwee, R. G., Howlett, A. C., Abood, M. E., Alexander, S. P. H., Di Marzo, V., Elphick, M. R., ... & Mechoulam, R. (2010). International Union of Basic and Clinical Pharmacology. LXXIX. Cannabinoid receptors and their ligands: beyond CB1 and CB2. *Pharmacological reviews*, *62*(4), 588-631. https://doi.org/10.1124/pr.110.003004

Pisanti, S., Malfitano, A. M., Ciaglia, E., Lamberti, A., Ranieri, R., Cuomo, G., ... & Laezza, C. (2017). Cannabidiol: State of the art and new challenges for therapeutic applications. *Pharmacology & therapeutics*, *175*, 133-150. https://doi.org/10.1016/j.pharmthera.2017.02.041

Ryberg, E., Larsson, N., Sjögren, S., Hjorth, S., Hermansson, N. O., Leonova, J., ... & Greasley, P. J. (2007). The orphan receptor GPR55 is a novel cannabinoid receptor. *British journal of*

pharmacology, *152*(7), 1092-1101. https://doi.org/10.1038/sj.bjp.0707460

Sacerdote, P., Martucci, C., Vaccani, A., Bariselli, F., Panerai, A. E., Colombo, A., ... & Massi, P. (2005). The nonpsychoactive component of marijuana cannabidiol modulates chemotaxis and IL-10 and IL-12 production of murine macrophages both in vivo and in vitro. *Journal of neuroimmunology*, *159*(1), 97-105. https://doi.org/10.1016/j.jneuroim.2004.10.003

Tanasescu, R., Gran, B., & Constantinescu, C. S. (2013). The endocannabinoid system: a revolving plate in neuro-immune interaction in health and disease. *Amino acids*, *45*(1), 95-112. https://doi.org/10.1007/s00726-012-1252-8

Thomas, A., Baillie, G. L., Phillips, A. M., Razdan, R. K., Ross, R. A., & Pertwee, R. G. (2007). Cannabidiol displays unexpectedly high potency as an antagonist of CB1 and CB2 receptor agonists in vitro. *British journal of pharmacology*, *150*(5), 613-623. https://doi.org/10.1038/sj.bjp.0707133

Vergara, D., Bidwell, L. C., Gaudino, R., Torres, A., Du, G., Ruthenburg, T. C., ... & Kane, N. C. (2017). Compromised External Validity: Federally Produced Cannabis Does Not Reflect Legal Markets. *Scientific reports*, *7*, 46528. https://doi.org/10.1101/083444

Walter, L., Franklin, A., Witting, A., Wade, C., Xie, Y., Kunos, G., ... & Stella, N. (2003). Nonpsychotropic cannabinoid receptors regulate microglial cell migration. *Journal of Neuroscience*, *23*(4), 1398-1405. https://doi.org/10.1523/jneurosci.23-04-01398.2003

Whyte, L. S., Ryberg, E., Sims, N. A., Ridge, S. A., Mackie, K., Greasley, P. J., ... & Rogers, M. J. (2009). The putative cannabinoid receptor GPR55 affects osteoclast function in vitro and bone mass in vivo. *Proceedings of the National Academy of Sciences*, *106*(38), 16511-16516. https://doi.org/10.1073/pnas.0902743106

Wilcox, R. R. (2012). *Introduction to Robust Estimation & Hypothesis Testing*. 3rd edition. Elsevier, Amsterdam, The Netherlands. https://doi.org/10.1016/c2010-0-67044-1

Xiong, W., Cui, T., Cheng, K., Yang, F., Chen, S. R., Willenbring, D., ... & Zhang, L. (2012). Cannabinoids suppress inflammatory and neuropathic pain by targeting α3 glycine receptors. *Journal of Experimental Medicine*, jem-20120242. https://doi.org/10.1084/jem.20120242

Yin, H., Chu, A., Li, W., Wang, B., Shelton, F., Otero, F., ... & Chen, Y. A. (2009). Lipid G protein-coupled receptor ligand identification using β-arrestin PathHunter™ assay. *Journal of Biological Chemistry*, *284*(18), 12328-12338. https://doi.org/10.1074/jbc.m806516200

Yung-Chi, C., & Prusoff, W. H. (1973). Relationship between the inhibition constant (Ki) and the concentration of inhibitor which causes 50 per cent inhibition (I50) of an enzymatic reaction. *Biochemical pharmacology*, *22*(23), 3099-3108. https://doi.org/10.1016/0006-2952(73)90196-2

Zuardi, A. W. (2008). Cannabidiol: from an inactive cannabinoid to a drug with wide spectrum of action. *Revista brasileira de psiquiatria*, *30*(3), 271-280. https://doi.org/10.1590/s1516-44462008000300015

Cultivar	Ultracentrifuged Inflorescence	Inflorescence	Petiole	Apical Bud/Leaf	Stalk
Uniko B	0.956	0.902	0.517	0.36	0.169
Kompolti	0.98	0.881	0.538	0.383	0.192
Fedora 17	0.976	0.865	0.52	0.43	0.191
Fedora 17	0.919	0.892	0.509	0.468	0.194
Fedora 17	0.95	0.907	0.569	0.409	0.201
Ferimon 12	0.92	0.866	0.517	0.392	0.19
Santhica 27	0.985	0.85	0.557	0.453	0.162
Epsilon 68	0.991	0.859	0.575	0.37	0.171
Futura 75	0.958	0.823	0.557	0.41	0.189
Futura 75	0.963	0.85	0.53	0.443	0.176
Felina 32	0.974	0.88	0.57	0.378	0.189
Felina 34	0.946	0.817	0.588	0.392	0.183
Juso 14	0.956	0.832	0.505	0.428	0.199
Bialobrzeskie	0.973	0.836	0.561	0.391	0.216
Beniko	0.984	0.844	0.516	0.434	0.175
Chamaeleon	0.969	0.85	0.525	0.384	0.17
Chamaeleon	0.972	0.907	0.513	0.397	0.226
Carmagnola	0.961	0.894	0.533	0.283	0.224
Carmagnola	0.973	0.862	0.565	0.431	0.21
Carmagnola selezionata	0.932	0.877	0.561	0.387	0.185
Tiborszallasi	0.94	0.882	0.531	0.359	0.192
Fibranova	0.974	0.893	0.51	0.408	0.23
Delta-llosa	0.949	0.852	0.54	0.397	0.228
Delta-405	0.982	0.858	0.561	0.378	0.179
Novgorod-Seversky, cv	0.947	0.888	0.569	0.393	0.204
Bernburgskaya Odnodomnaya, bm	0.97	0.805	0.552	0.385	0.193
Szegedi 9	0.936	0.88	0.521	0.373	0.166
Fibrimulta 151	0.971	0.876	0.531	0.358	0.189

Glukhovskaya 10 Zheltostebel'naya	0.989	0.807	0.554	0.378	0.192
Krasnodarsky 10 FB	0.965	0.876	0.576	0.43	0.191
Alpine Rocket	0.951	0.841	0.62	0.427	0.198
Alpine Rocket	0.947	0.79	0.517	0.436	0.206
Hindu Kush	0.935	0.887	0.529	0.425	0.183
Northern Light	0.993	0.871	0.546	0.36	0.221
Snow White	0.931	0.817	0.506	0.349	0.159
Top 44	0.973	0.839	0.515	0.38	0.189
Top 44	0.934	0.861	0.553	0.325	0.188
F1 Fraise	0.966	0.863	0.514	0.431	0.197
B52	0.943	0.914	0.543	0.429	0.226
Peace Maker	0.946	0.848	0.534	0.346	0.197
Big Bud	0.951	0.9	0.536	0.379	0.2
Big Skunk	0.967	0.867	0.509	0.369	0.184
F Fraise	0.931	0.875	0.517	0.405	0.213
Hawaii Maui Waui	0.985	0.84	0.485	0.382	0.194
Haze	0.993	0.884	0.596	0.457	0.158
Swaziland	0.981	0.834	0.579	0.397	0.192
Mexican Sativa	0.963	0.825	0.528	0.451	0.207
Ruderalis Indica	0.942	0.789	0.499	0.398	0.186

Appendix 1: 48 cultivars of cannabis, and their associated bioactivity levels by plant organ.

Cultivar	Ultracentrifuged Inflorescence	Inflorescence	Petiole	Apical Bud/Leaf	Stalk
H. Kriya #3	0.964	0.829	0.536	0.465	0.212
H. Kriya #5	0.947	0.798	0.532	0.414	0.195
H. Kriya #6	0.956	0.883	0.549	0.399	0.215
H. Kriya #11	0.961	0.96	0.551	0.445	0.188
H. Kriya #14	0.941	0.835	0.519	0.402	0.21
H. Kriya #17	0.932	0.851	0.536	0.355	0.182

Appendix 2: 6 samples of ImmunAG, and their associated bioactivity levels by plant organ.

Volume 1, Article 3; Pages 26-28 Doi: 10.31013/2002a

Editorial

Towards systematically assessing bioactivity of natural compounds or bio-ligands: Cannabidiol as an example

D. Cushing[1]* & B. Joseph[1]

[1]: Peak Health Center, Los Gatos, CA

*For inquiries, email corresponding author at donish@peakhealth.center

Recieved: June 20, 2018

Accepted: June 20, 2018

Published: June 26, 2018

Citation: Cushing, C., Joseph, B. (2018b). Towards systematically assessing bioactivity of natural compounds or bio-ligands: Cannabidiol as an example. Retrieved from https://doi.org/10.31013/2002c

Western medicine by law requires that drugs be synthetic compounds which are mass produced in heavily controlled manufacturing environments. In recent years there has been increasing interest in complementary and alternative medicine (CAM) for treating disease in the United States (e.g., White et al., 2017). Natural, non-vitamin, non-mineral dietary supplements account for a sizeable share of these approaches (17.7% in Clarke, Black, Stussman, Barnes, & Nahin, 2015). Despite their potential efficacy, a very small proportion of patients in the United States use CAM methods as complete replacements for standard pharmaceutical treatment (Nahin, Dahlhamer, & Stussman, 2010). Most CAM users reported taking natural dietary supplements for general wellness and preventative healthcare rather than specific outcomes (Marinac, Buchinger, Godfrey, Wooten, Sun, & Willsie, 2007). One reason is that identifying the dosages required for medicinal plant-derived compounds to treat specific diseases has proven difficult.

This was the case with cannabidiol (CBD). The CB2 receptor is a G-coupled protein receptor located predominantly in immune cells whose distribution and functions coincide closely with many observed immune effects of CBD (Ligresti, De Petrocellis, & Di Marzo, 2016). Despite hundreds of scientific articles written about CBD in recent times (Burstein, 2015; Zuardi, 2008), published displacement values (K_i) for the CBD/CB_2 interaction continue to vary substantially. Inconsistent results such as these make dosage recommendations impossible (Thomas, 2017). To solve this problem, a novel approach was developed to predict CBD/CB2 binding affinity between samples (Cushing, Kristipati, Shastri, and Joseph, 2018). Plant source and processing factors were identified to alter CB2 receptor affinity of CBD.

It is estimated that 75-78% of all modern medicines are directly or indirectly derived from higher plants (Samuelsson, 2004). Less than 5% of all plant species have been explored for their medical potential (Chin, Balunas, Chai, & Kinghorn, 2006). Natural plant compounds rarely have side effects. This makes them a potent alternative to pharmaceutical drugs for chronic use.

All active ingredients from plants are biological molecules. They have a complex biochemical pathway to produce a somatic effect on the human body. In order for plant materials to rival pharmaceutical drugs, they have to

undergo the same pharmaceutical factors – namely measurement of its bioactivity, knowledge of its pharmacokinetic and pharmacodynamic properties, and standardized quantities of active ingredient with the indential bioactive properties.

A three-step process for measuring bioactivity of all samples from natural plant-based sources will is outlined, using CBD as an example. This process is paramount for the application of natural plant-based compounds in western medicine.

3 steps for systematically assessing bioactivity:

The first step is to identify an important mechanism by which the compound studied acts on the body. In the case of CBD, decades of research have revealed multiple receptor targets. CB2 remains the most abundant cannabinoid receptor in the human body, and so it was the target of investigation by Cushing et al. (2018).

The second step is to develop a test that can compare the active compound from various samples. In most cases, direct tests of the mechanism of action are cumbersome. In these situations, scientists need to devise clever workarounds. CBD produces an indirect antagonistic effect on CB2 agonists WIN55212-2 and CP55290. In a binding assay, this antagonism can be measured using Chinese Hamster Ovary (CHO) cells with recombinant CB2 receptors. However, CHO membrane lines are expensive to generate, maintain, and test. So their use as a functional rapid tester for large quantities of CBD, over extended periods, is not practical. The experiment described in Cushing et al. utilized a Monoclonal Antibody (MCA) that displayed binding affinities to the CBD molecule with values that correlated highly (r = .97) to CB2 WIN55212-2 displacement values. This test was also simple to conduct. With such a high correlation, it became reasonable to predict CB2 affinity (and thus, bioactivity) with this more efficient MCA-based test.

The third step is to test samples for adequate bioactivity. In the case of CBD, Cushing et al. found that cannabis-based commercial samples had unanimously very low bioactivity compared to the ideal. This allowed them to issue a warning that standard commercial CBD samples should not be used for medical trials. Only tested products with high bioactivity should be used in medical studies.

To summarize, the three steps are as follows:

1) Identify the mechanism of action that relates to the bioactivity of the molecules.

2) Develop a test by which the bioactivity of the molecule can be measured.

3) Test commercial samples on a mass scale.

This three step process should be applied to all biological phyto compounds that have efficacy in the human body. Poor processing, pyrolysis, biodegradation, plant origin, and storage conditions can all affect the bioactivity of natural compounds. Research is undermined when it unwittingly uses low bioactivity samples. Knowing the bioactivity of an organic molecule is a key element in knowing its quality and functionality.

Conclusion:

It is estimated that 70-95% of the population in developing countries continues to use traditional medicines (Robinson & Zhang, 2011). Medical professionals in developed nations should account for natural plant ingredients as therapeutic agents. To this end, systematic control of factors that underlie variation in the bioactivity of natural plant compounds is paramount. A successful approach to testing the bioactivity of CBD between samples has been demonstrated. The same approach can be extended to natural medicinal compounds of all types. This extension has the potential to change the medical landscape globally, opening up a new frontier in western medicine.

References:

Burstein, S. (2015). Cannabidiol (CBD) and its analogs: a review of their effects on inflammation. *Bioorganic & medicinal chemistry*, *23*(7), 1377-1385. https://doi.org/10.1016/j.bmc.2015.01.059

Chin, Y. W., Balunas, M. J., Chai, H. B., & Kinghorn, A. D. (2006). Drug discovery from natural sources. *The AAPS journal*, *8*(2), E239-E253. https://doi.org/10.1201/b11196-12

Clarke, T. C., Black, L. I., Stussman, B. J., Barnes, P. M., & Nahin, R. L. (2015). Trends in the use of complementary health approaches among adults: United States, 2002–2012. *National health statistics reports*, (79), 1.

Ligresti, A., De Petrocellis, L., & Di Marzo, V. (2016). From phytocannabinoids to cannabinoid receptors and endocannabinoids: pleiotropic physiological and pathological roles through complex pharmacology. *Physiological reviews*, *96*(4), 1593-1659. https://doi.org/10.1152/physrev.00002.2016

Marinac, J. S., Buchinger, C. L., Godfrey, L. A., Wooten, J. M., Sun, C., & Willsie, S. K. (2007). Herbal products and dietary supplements: a survey of use, attitudes, and knowledge among older adults. *The Journal of the American Osteopathic Association*, *107*(1), 13-23.

Nahin, R. L., Dahlhamer, J. M., & Stussman, B. J. (2010). Health need and the use of alternative medicine among adults who do not use conventional medicine. *BMC Health Services Research*, *10*(1), 220. https://doi.org/10.1186/1472-6963-10-220

Robinson, M. M., and Zhang, X (2011). The World Medicines Situation 2011. Traditional Medicines: Global Situation, Issues and Challenges, Geneya: World Health Organization.

Samuelsson, G. (ed.). (2004). *Drugs of Natural Origin: A Textbook of phamacognosy*, 5th Edn Stockholrn: Swedish Pharmaceutical Press.

Thomas, B. F. (2017). Cannabidiol as a Treatment for Seizures, Convulsions and Epilepsy. In *Cannabis sativa L.-Botany and Biotechnology* (pp. 249-261). Springer, Cham. https://doi.org/10.1007/978-3-319-54564-6_11

White, J. D., O'Keefe, B. R., Sharma, J., Javed, G., Nukala, V., Ganguly, A., ... & Walker, L. (2017). India-United States Dialogue on Traditional Medicine: Toward Collaborative Research and Generation of an Evidence Base. *Journal of Global Oncology*, JGO-17. https://doi.org/10.1200/jgo.17.00099

Zuardi, A. W. (2008). Cannabidiol: from an inactive cannabinoid to a drug with wide spectrum of action. *Revista brasileira de psiquiatria*, *30*(3), 271-280. https://doi.org/10.1590/s1516-44462008000300015

Volume 1, Article 4; Pages 29-47 Doi: 10.31013/2002a

Data Report

Identification of cannabidiol from Humulus Kriya using x-ray crystallography

D. Cushing[1]* & B. Joseph[1]

[1]: Peak Health Center, Los Gatos, CA

*For inquiries, email corresponding author at donish@peakhealth.center

Recieved: June 19, 2018

Accepted: June 20, 2018

Published: June 26, 2018

Citation: Cushing, C., Joseph, B. (2018c). Identification of cannabidiol from Humulus Kriya using x-ray crystallography. Retrieved from https://doi.org/10.31013/2002d

Abstract

The crystal structure of cannabidiol, was determined by the application of Cu *Kf3* radiation single-crystal X-ray crystallography. The unsaturated alkyl chain of the cannabidiol molecule was found to be freely rotatable. We found two molecules with different orientations ofthis side chain within the asymmetric unit. These independent molecules are both found to have the R,R configuration, just like cannabidiol from *Cannabis Sativa*.

The crystal structure of cannabidiol, C21H30O2, {2-[(1R,6R)-3-methyl-6-(prop-1-en-2-yl)cyclohex-2-enyl]-5-pentylbenzene-1,3-diol}, was first determined by Jones et al. (1977) and Ottersen & Rosenqvist (1977). Mechoulam (1967) identified and represented the structure as *R,R* by chemical means, which was a laborious and remarkable feat.

We used advanced single-crystal X-ray diffractometers to study the structure of a fraction isolated from the Humulus kriya plant. The unique Cu Kf3 wavelength radiation determined that the absolute structure was *R,R*— the same as the Cannabidiol structure represented by Mechoulam. We found an identical crystal structure to CBD from cannabis sativa (Mayr, Grassl, Korber, Christoffel & Bodensteiner, 2017).

Procedure

The crystal structure of cannabidiol, (Figure 1), was determined by the application of Cu Kf3 radiation

single-crystal X-ray crystallography. This is a rather uncommon wavelength radiation to measure crystal structures. The unsaturated alkyl chain of the cannabidiol molecule was found to be freely rotatable. We found two molecules with different orientations of this side chain within the asymmetric unit (Figures 2 & 3). These independent molecules are both found to have the *R,R* configuration, confirming earlier investigations by Jones *et al.* (1977), Ottersen & Rosenqvist (1977) and Mechoulam *et al.* (1967).

Synthesis and crystallization

Cannabidiol was obtained from ImmunAG LLP, 501, Edcon Mindspace, Campal, Panaji, Goa, India-403001. *n*-Heptane was used to recrystallize the Cannabidiol and further purify it. The crystal was selected using standard preparation techniques, and mounted on a MiTiGen-loop using mineral oil.

Refinement

Crystallographic data, data collection and strucutre refinement details are summarized in Table 1.

Crystal data	
Chemical formula	C21H30O2
M*r*	314.45
Crystal system, space group	Monoclinic, $P2_1$
Temperature (K)	123
a, b, c (Ä)	10.4395 (1), 10.8739 (1), 16.7853 (2)
ß (o)	95.448 (1)
V (Å^3)	1896.83 (3)
Z	4
Radiation type	Cu *Kß*
μ (mm^{-1})	0.39
Crystal size (mm)	0.28 X 0.16 X 0.15
Data collection	
Diffractometer	Agilent GV1000, TitanS2
Absorption correction	Gaussian (*CrysAlis* PRO; Rigaku OD, 2015)
T_{min}, T_{max}	0.996, 0.997
No. of measured, independent and observed [$I > 2\sigma$-(I)] reflections	85198, 10203, 9859
Rint	0.044
(sin θ/λ)max (Å -1)	0.695
Refinement	
R[F 2 > 2o-(F 2)], wR(F 2), S	0.032, 0.088, 1.03
No. of reflections	10203
No. of parameters	655
No. of restraints	1
H-atom treatment	All H-atom parameters refined
$\Delta\rho_{max}$, $\Delta\rho_{min}$ (e Å^{-3})	0.23, 0.13
Absolute structure	Flack *x* determined using 4335 quotients [(I^+) - (I^-)]/[(I^+)+(I^-)] (Parsons et al., 2013)
Absolute structure parameter	-0.03 (6)

Table 1: Experimental details.

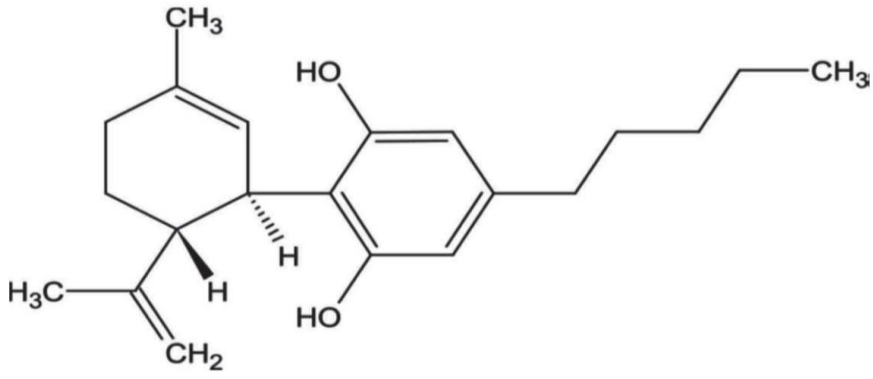

Figure 2: 3-D structure of Cannabidiol isolated from H kriya

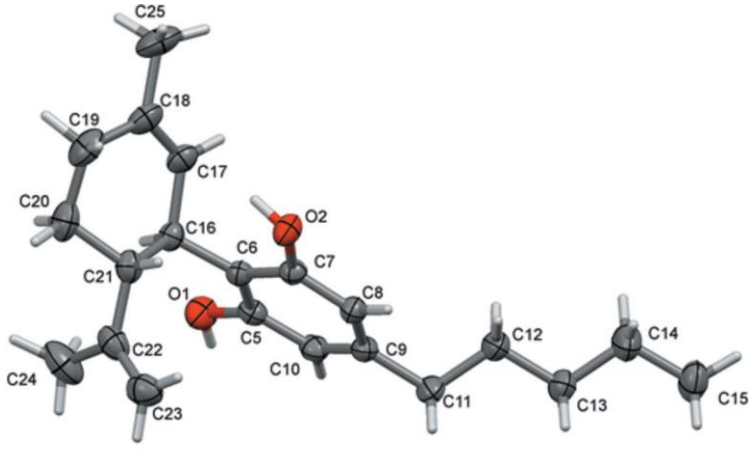

Fig 3: 3-D structure of one independent Cannabidiol molecule isolated from H kriya

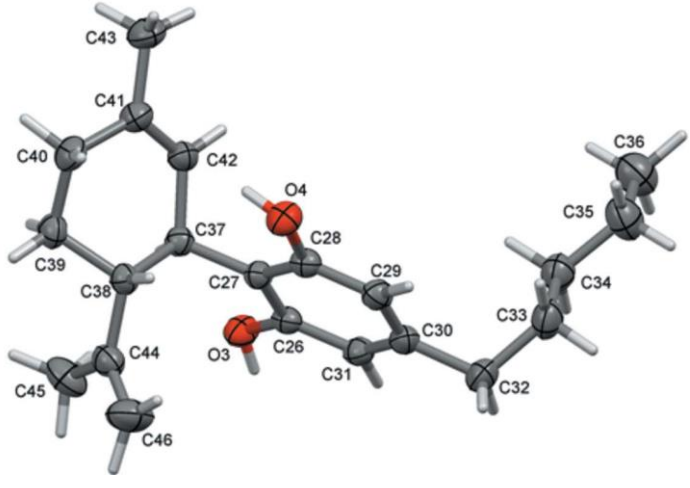

Fig 4: 3-D structure of a second independent Cannabidiol molecule isolated from H kriya

References:

Dolomanov, O. V., Bourhis, L. J., Gildea, R. J., Howard, J. A., & Puschmann, H. (2009). OLEX2: a complete structure solution, refinement and analysis program. *Journal of Applied Crystallography*, *42*(2), 339-341. https://doi.org/10.1107/s0021889808042726

Jones, P. G., Falvello, L., Kennard, O., Sheldrick, G. M., & Mechoulam, R. (1977). Cannabidiol. *Acta Crystallographica Section B: Structural Crystallography and Crystal Chemistry*, *33*(10), 3211-3214. https://doi.org/10.1107/s0567740877010577

Macrae, C.F., Bruno, I.J., Chisholm, J.A., Edgington, P.R., McCabe, P., Pidcock, E., ... & Wood, P.A. (2008) New Features for the Visualization and Investigation of Crystal Structures. *Journal of Applied Crystallography, 41*, 466-470. http://dx.doi.org/10.1107/S0021889807067908

Mayr, T., Grassl, T., Korber, N., Christoffel, V., & Bodensteiner, M. (2017). Cannabidiol revisited. *IUCrData*, *2*(2), x170276. https://doi.org/10.1107/s2414314617002760

Mechoulam, R., Braun, P., & Gaoni, Y. (1967). Stereospecific synthesis of (-)-. DELTA. 1-and (-)-. DELTA. 1 (6)-tetrahydrocannabinols. *Journal of the American Chemical Society*, *89*(17), 4552-4554. https://doi.org/10.1021/ja00993a072

Ottersen, T. & Rosenqvist, E. (1977). The crystal and molecular structure of cannabidiol. *Acta Chem. Scand.* 31b, 749– 755. https://doi.org/10.3891/acta.chem.scand.31b-0807

Parsons, S., Flack, H. D., & Wagner, T. (2013). Use of intensity quotients and differences in absolute structure refinement. *Acta Crystallographica Section B: Structural Science, Crystal Engineering and Materials*, *69*(3), 249-259. https://doi.org/10.1107/s2052519213010014

Sheldrick, G. M. (2015). Crystal structure refinement with SHELXL. *Acta Crystallographica Section C: Structural Chemistry*, *71*(1), 3-8.

Full crystallographic report

Crystal data

$C_{21}H_{30}O_2$
M_r = 314.45
Monoclinic, $P2_1$
a = 10.4395 (1) Å
b = 10.8739 (1) Å
c = 16.7853 (2) Å
$ß$ = 95.448 (1)º
V = 1896.83 (3) Å^3
Z = 4
F(000) = 668

D_x = 1.101 mg m^{-3}
Melting point = 339-340 K
Cu $Kß$ radiation, λ = 1.39222 Å
Cell parameters from 54306 reflections
θ = 3.6-74.8º
μ = 0.39 mm^{-1}
T = 123 K
Prism, clear colorless

Data collection

Agilent GV1000, TitanS2 diffractometer
Radiation source: gradient vacuum rotating-anode X-ray tube, GV1000 (Cu) X-ray sourcec
Mirror monochromator
Detector resolution: 4.1818 pixels mm^{-1}
ω scans
Absorption correction: gaussian (CrysAlisPro; Rigaku OD, 2015)

T_{min} = 0.996, T_{max} = 0.997
85198 measured reflections
9859 reflections with $I > 2\sigma(I)$
R_{int} = 0.044
θ_{max} = 75.3º, θ_{min} = 2.4º
h = -14 → 14
k = -15 → 14
l = -23 → 23

Refinement

Refinement on F^2
Least-squares matrix: full
$R[F^2 > 2\sigma(F^2)]$ = 0.032
$wR(F^2)$ = 0.088
S = 1.03
10203 reflections
655 parameters
1 restraint
Primary atom site location: dual
Hydrogen site location: difference Fourier map
Special details

All H-atom paramaters refined
$w = 1/[\sigma^2(F^2) + (0.0493P)^2 + 0.1553P]$ where $P = (F^2 + 2F^2)/3$
$(\Delta/\sigma)_{max} < 0.001$
$\Delta\rho_{max}$ = 0.23 e Å^{-3}
$\Delta\rho_{min}$ = −0.13 e Å^{-3}
Absolute structure: Flack x determined using 4335 quotients $[(I^+)-(I^-)]/[(I^+)+(I^-)]$ (Parsons *et al.,* *2013)*
Absolute structure parameter: -0.03 (6)

Fractional atomic coordinates and isotropic or equivalent isotropic displacement parameters (Å^2)

	x	*y*	*z*	U_{iso}*/U_{eq}
O2	0.45873 (9)	0.27113 (11)	0.68801 (7)	0.0350 (2)
O3	0.22910 (10)	0.31909 (11)	0.75679 (7)	0.0361 (2)
O4	−0.01007 (11)	0.64952 (12)	0.85698 (7)	0.0370 (2)
O1	0.89037 (10)	0.39186 (12)	0.65474 (7)	0.0401 (2)
C7	0.56191 (12)	0.35049 (13)	0.70250 (8)	0.0280 (2)
C27	0.11199 (12)	0.47899 (13)	0.81028 (7)	0.0276 (2)
C28	0.06220 (12)	0.59824 (14)	0.80142 (8)	0.0298 (2)
C26	0.18235 (11)	0.43560 (13)	0.74901 (7)	0.0285 (2)
C6	0.68036 (12)	0.32428 (13)	0.67315 (7)	0.0272 (2)
C5	0.77497 (12)	0.41511 (14)	0.68514 (8)	0.0297 (2)
C29	0.08240 (13)	0.67195 (14)	0.73595 (9)	0.0337 (3)
C41	−0.10203 (14)	0.40126 (16)	0.96293 (9)	0.0360 (3)
C37	0.09170 (12)	0.39998 (14)	0.88271 (7)	0.0290 (2)
C9	0.63810 (13)	0.54375 (14)	0.75803 (8)	0.0317 (3)
C16	0.70534 (12)	0.20447 (14)	0.63181 (8)	0.0301 (2)
C8	0.54143 (13)	0.45499 (14)	0.74650 (8)	0.0309 (2)
C10	0.75383 (13)	0.52378 (14)	0.72519 (8)	0.0328 (3)
C38	0.16926 (12)	0.44801 (14)	0.96000 (8)	0.0309 (3)
C31	0.20157 (13)	0.50812 (15)	0.68246 (8)	0.0327 (3)
C42	−0.05071 (13)	0.39038 (15)	0.89332 (8)	0.0329 (3)
C30	0.15332 (13)	0.62697 (15)	0.67583 (8)	0.0334 (3)
C17	0.61190 (15)	0.18610 (16)	0.55797 (8)	0.0359 (3)
C18	0.56273 (18)	0.07793 (18)	0.53315 (9)	0.0432 (4)
C44	0.31309 (14)	0.43548 (17)	0.95708 (9)	0.0381 (3)
C21	0.70272 (14)	0.09214 (15)	0.68849 (9)	0.0352 (3)
C22	0.80132 (16)	0.10349 (17)	0.76024 (11)	0.0426 (3)

C11	0.61657 (16)	0.66019 (16)	0.80361 (10)	0.0390 (3)
C39	0.12060 (15)	0.38200 (17)	1.03236 (8)	0.0374 (3)
C32	0.17722 (17)	0.70713 (19)	0.60483 (10)	0.0434 (4)
C12	0.49874 (18)	0.73187 (17)	0.77039 (10)	0.0429 (3)
C33	0.0558 (2)	0.74656 (19)	0.55280 (11)	0.0475 (4)
C40	−0.01885 (16)	0.41677 (18)	1.04074 (9)	0.0408 (3)
C13	0.47857 (18)	0.85021 (16)	0.81437 (10)	0.0414 (3)
C23	0.7641 (2)	0.12371 (19)	0.83228 (11)	0.0498 (4)
C20	0.7152 (2)	−0.02482 (18)	0.63891 (13)	0.0494 (4)
C43	−0.24537 (17)	0.3974 (2)	0.96703 (12)	0.0503 (4)
C34	−0.01477 (18)	0.64082 (19)	0.50915 (11)	0.0449 (4)
C14	0.3597 (2)	0.9199 (2)	0.78214 (16)	0.0630 (6)
C25	0.4721 (3)	0.0678 (3)	0.45807 (12)	0.0607 (6)
C45	0.36871 (18)	0.3090 (2)	0.95561 (14)	0.0528 (5)
C46	0.38685 (19)	0.5344 (3)	0.95736 (16)	0.0603 (5)
C19	0.5994 (2)	−0.03921 (19)	0.57671 (13)	0.0540 (4)
C15	0.3401 (2)	1.0401 (2)	0.82410 (13)	0.0543 (5)
C35	−0.1338 (2)	0.6820 (2)	0.45576 (15)	0.0578 (5)
C24	0.9415 (2)	0.0943 (3)	0.74624 (18)	0.0663 (6)

C36	−0.1995 (2)	0.5757 (3)	0.40974 (17)	0.0636 (6)
H40A	−0.025 (2)	0.504 (2)	1.0609 (14)	0.043 (5)*
H38	0.1488 (18)	0.538 (2)	0.9650 (11)	0.027 (4)*
H8	0.459 (2)	0.466 (2)	0.7688 (13)	0.042 (5)*
H33A	−0.005 (3)	0.789 (3)	0.5860 (17)	0.062 (7)*
H39A	0.177 (2)	0.401 (2)	1.0813 (13)	0.041 (5)*
H21	0.617 (2)	0.089 (2)	0.7084 (12)	0.033 (5)*
H33B	0.085 (3)	0.807 (3)	0.5148 (17)	0.063 (8)*
H19A	0.527 (3)	−0.071 (3)	0.6008 (16)	0.060 (7)*
H42	−0.107 (2)	0.374 (2)	0.8461 (12)	0.035 (5)*
H32A	0.235 (3)	0.665 (3)	0.5677 (16)	0.055 (7)*
H37	0.1249 (18)	0.315 (2)	0.8712 (11)	0.030 (4)*
H16	0.7917 (18)	0.210 (2)	0.6121 (11)	0.030 (4)*
H39B	0.127 (2)	0.290 (3)	1.0247 (14)	0.046 (6)*
H40B	−0.055 (2)	0.365 (3)	1.0835 (15)	0.050 (6)*
H17	0.591 (2)	0.264 (3)	0.5272 (15)	0.047 (6)*
H31	0.251 (2)	0.476 (2)	0.6408 (13)	0.043 (5)*
H45A	0.356 (4)	0.256 (4)	1.004 (2)	0.092 (11)*
H20A	0.798 (3)	−0.018 (3)	0.6132 (16)	0.060 (7)*
H34A	−0.042 (2)	0.578 (3)	0.5498 (15)	0.050 (6)*
H10	0.823 (2)	0.585 (2)	0.7311 (13)	0.039 (5)*
H11A	0.608 (2)	0.639 (3)	0.8615 (15)	0.050 (6)*
H13A	0.550 (3)	0.902 (3)	0.8117 (18)	0.069 (8)*
H1	0.943 (3)	0.444 (3)	0.6727 (15)	0.054 (7)*
H13B	0.473 (3)	0.835 (3)	0.8723 (17)	0.058 (7)*
H29	0.049 (2)	0.756 (2)	0.7327 (13)	0.043 (6)*
H24A	0.961 (3)	0.150 (3)	0.7046 (19)	0.070 (8)*
H24B	0.993 (3)	0.106 (3)	0.793 (2)	0.077 (9)*
H3	0.290 (2)	0.307 (2)	0.7284 (14)	0.046 (6)*
H35A	−0.111 (3)	0.746 (3)	0.4193 (18)	0.063 (8)*
H35B	−0.190 (3)	0.721 (3)	0.4888 (19)	0.068 (8)*
H46A	0.483 (3)	0.524 (3)	0.9616 (18)	0.071 (9)*

H43A	−0.283 (3)	0.469 (3)	0.9898 (19)	0.074 (9)*
H12A	0.416 (3)	0.679 (3)	0.7686 (19)	0.073 (9)*
H46B	0.344 (4)	0.613 (4)	0.958 (2)	0.090 (11)*
H12B	0.499 (3)	0.750 (3)	0.7153 (19)	0.070 (8)*
H15A	0.342 (3)	1.031 (3)	0.883 (2)	0.080 (10)*
H19B	0.617 (3)	−0.104 (3)	0.537 (2)	0.074 (9)*
H32B	0.223 (3)	0.781 (3)	0.6257 (17)	0.064 (8)*
H14A	0.365 (4)	0.935 (4)	0.720 (3)	0.113 (14)*
H34B	0.048 (2)	0.596 (3)	0.4745 (15)	0.052 (6)*
H20B	0.721 (3)	−0.098 (3)	0.6747 (16)	0.057 (7)*
H43B	−0.293 (3)	0.386 (3)	0.9146 (17)	0.060 (7)*
H23A	0.676 (3)	0.132 (3)	0.8403 (16)	0.059 (7)*
H23B	0.818 (3)	0.130 (3)	0.8784 (17)	0.061 (7)*
H2	0.475 (2)	0.223 (2)	0.6496 (14)	0.044 (5)*
H4	−0.036 (3)	0.593 (3)	0.8864 (16)	0.054 (7)*
H43C	−0.264 (3)	0.331 (3)	1.0030 (19)	0.073 (9)*

H25A	0.443 (3)	0.156 (4)	0.438 (2)	0.075 (9)*
H15B	0.415 (3)	1.097 (4)	0.815 (2)	0.082 (10)*
H36A	−0.142 (3)	0.538 (3)	0.3720 (17)	0.063 (8)*
H25B	0.512 (3)	0.020 (3)	0.4207 (19)	0.069 (8)*
H25C	0.401 (3)	0.024 (3)	0.4684 (19)	0.073 (9)*
H45B	0.463 (3)	0.312 (3)	0.9515 (18)	0.068 (8)*
H11B	0.692 (3)	0.713 (3)	0.8057 (18)	0.072 (8)*
H45C	0.331 (3)	0.264 (3)	0.914 (2)	0.078 (9)*
H36B	−0.222 (3)	0.515 (4)	0.448 (2)	0.076 (9)*
H14B	0.280 (5)	0.877 (5)	0.788 (3)	0.125 (16)*
H36C	−0.284 (4)	0.611 (4)	0.377 (2)	0.088 (11)*
H24C	0.955 (4)	0.003 (4)	0.723 (2)	0.093 (11)*
H15C	0.261 (4)	1.085 (4)	0.808 (2)	0.098 (12)*

Atomic displacement parameters (Å^2)

	U^{11}	U^{22}	U^{33}	U^{12}	U^{13}	U^{23}
O2	0.0289 (4)	0.0337 (5)	0.0438 (5)	−0.0053 (4)	0.0102 (4)	−0.0110 (4)
O3	0.0349 (5)	0.0343 (6)	0.0409 (5)	0.0056 (4)	0.0121 (4)	−0.0004 (4)
O4	0.0416 (5)	0.0330 (6)	0.0380 (5)	0.0046 (4)	0.0113 (4)	−0.0038 (4)
O1	0.0277 (4)	0.0454 (7)	0.0481 (6)	−0.0063 (4)	0.0074 (4)	−0.0059 (5)
C7	0.0276 (5)	0.0280 (6)	0.0281 (5)	−0.0018 (4)	0.0016 (4)	−0.0003 (4)

C27	0.0256 (5)	0.0302 (6)	0.0271 (5)	−0.0014 (4)	0.0027 (4)	−0.0013 (4)
C28	0.0273 (5)	0.0313 (7)	0.0309 (5)	−0.0008 (5)	0.0034 (4)	−0.0028 (5)
C26	0.0237 (5)	0.0316 (7)	0.0302 (5)	−0.0003 (4)	0.0027 (4)	−0.0026 (5)
C6	0.0277 (5)	0.0279 (6)	0.0258 (5)	0.0000 (4)	0.0018 (4)	0.0007 (4)
C5	0.0264 (5)	0.0331 (7)	0.0292 (5)	−0.0011 (5)	0.0003 (4)	0.0028 (5)
C29	0.0312 (6)	0.0311 (7)	0.0386 (6)	−0.0008 (5)	0.0028 (5)	0.0025 (5)
C41	0.0335 (6)	0.0392 (8)	0.0361 (6)	−0.0019 (5)	0.0077 (5)	0.0030 (6)
C37	0.0297 (5)	0.0301 (7)	0.0272 (5)	−0.0006 (5)	0.0032 (4)	−0.0002 (4)
C9	0.0332 (6)	0.0290 (7)	0.0314 (6)	0.0017 (5)	−0.0052 (5)	−0.0027 (5)
C16	0.0300 (6)	0.0299 (7)	0.0312 (5)	0.0007 (5)	0.0075 (4)	−0.0016 (5)
C8	0.0294 (5)	0.0315 (7)	0.0315 (5)	0.0020 (5)	0.0014 (4)	−0.0037 (5)
C10	0.0300 (6)	0.0306 (7)	0.0361 (6)	−0.0033 (5)	−0.0049 (5)	−0.0003 (5)
C38	0.0311 (6)	0.0330 (7)	0.0282 (5)	−0.0004 (5)	0.0016 (4)	−0.0004 (5)
C31	0.0277 (5)	0.0415 (8)	0.0294 (5)	−0.0034 (5)	0.0061 (4)	−0.0021 (5)
C42	0.0314 (6)	0.0358 (7)	0.0315 (6)	−0.0042 (5)	0.0026 (5)	0.0016 (5)
C30	0.0295 (6)	0.0394 (8)	0.0311 (6)	−0.0056 (5)	0.0015 (4)	0.0042 (5)
C17	0.0409 (7)	0.0392 (8)	0.0285 (6)	−0.0005 (6)	0.0084 (5)	−0.0053 (5)
C18	0.0503 (8)	0.0465 (10)	0.0342 (6)	−0.0056 (7)	0.0112 (6)	−0.0129 (6)
C44	0.0331 (6)	0.0473 (9)	0.0332 (6)	0.0020 (6)	−0.0008 (5)	−0.0012 (6)
C21	0.0356 (6)	0.0301 (7)	0.0405 (7)	0.0012 (5)	0.0070 (5)	0.0011 (5)
C22	0.0397 (7)	0.0357 (8)	0.0513 (8)	0.0028 (6)	−0.0013 (6)	0.0103 (7)
C11	0.0403 (7)	0.0319 (8)	0.0426 (7)	0.0032 (6)	−0.0069 (6)	−0.0098 (6)
C39	0.0414 (7)	0.0435 (9)	0.0271 (5)	0.0016 (6)	0.0020 (5)	0.0031 (5)
C32	0.0429 (7)	0.0482 (10)	0.0393 (7)	−0.0094 (7)	0.0051 (6)	0.0112 (7)
C12	0.0493 (8)	0.0349 (8)	0.0423 (8)	0.0082 (6)	−0.0073 (6)	−0.0079 (6)

C33	0.0572 (9)	0.0442 (10)	0.0403 (8)	−0.0047 (7)	0.0011 (7)	0.0111 (7)
C40	0.0433 (7)	0.0491 (10)	0.0311 (6)	−0.0003 (6)	0.0093 (5)	0.0014 (6)
C13	0.0501 (8)	0.0306 (8)	0.0427 (7)	0.0049 (6)	0.0006 (6)	−0.0046 (6)
C23	0.0590 (10)	0.0435 (10)	0.0448 (8)	−0.0022 (8)	−0.0065 (7)	0.0068 (7)
C20	0.0574 (10)	0.0300 (8)	0.0621 (10)	0.0052 (7)	0.0128 (8)	−0.0040 (7)
C43	0.0355 (7)	0.0689 (13)	0.0484 (8)	−0.0037 (8)	0.0136 (6)	0.0041 (9)
C34	0.0488 (8)	0.0426 (9)	0.0429 (8)	−0.0007 (7)	0.0022 (6)	0.0068 (7)
C14	0.0641 (12)	0.0452 (12)	0.0756 (14)	0.0181 (9)	−0.0141 (10)	−0.0167 (10)
C25	0.0731 (13)	0.0685 (15)	0.0401 (8)	−0.0155 (11)	0.0037 (9)	−0.0236 (9)
C45	0.0413 (8)	0.0558 (12)	0.0591 (10)	0.0145 (8)	−0.0063 (7)	−0.0074 (9)
C46	0.0366 (8)	0.0613 (14)	0.0833 (15)	−0.0080 (8)	0.0070 (9)	0.0000 (11)
C19	0.0686 (12)	0.0369 (10)	0.0577 (10)	−0.0088 (8)	0.0122 (9)	−0.0156 (8)
C15	0.0680 (12)	0.0384 (10)	0.0581 (10)	0.0133 (9)	0.0143 (9)	−0.0006 (8)
C35	0.0599 (11)	0.0511 (12)	0.0593 (11)	0.0042 (9)	−0.0112 (9)	0.0052 (9)
C24	0.0396 (9)	0.0783 (17)	0.0794 (15)	0.0108 (10)	−0.0016 (9)	0.0226 (14)
C36	0.0584 (12)	0.0607 (14)	0.0692 (13)	0.0005 (10)	−0.0070 (10)	0.0006 (11)

Geometric parameters (Å, º)

O2—C7	1.3836 (16)	C11—H11B	0.98 (3)
O2—H2	0.86 (3)	C39—C40	1.523 (2)
O3—C26	1.3595 (18)	C39—H39A	0.98 (2)
O3—H3	0.84 (3)	C39—H39B	1.02 (3)

O4—C28	1.3723 (16)	C32—C33	1.531 (3)
O4—H4	0.85 (3)	C32—H32A	1.02 (3)
O1—C5	1.3756 (17)	C32—H32B	0.98 (3)
O1—H1	0.83 (3)	C12—C13	1.508 (2)
C7—C6	1.4031 (18)	C12—H12A	1.03 (3)
C7—C8	1.3829 (19)	C12—H12B	0.95 (3)
C27—C28	1.400 (2)	C33—C34	1.516 (3)
C27—C26	1.4011 (17)	C33—H33A	1.00 (3)
C27—C37	1.5198 (18)	C33—H33B	0.99 (3)
C28—C29	1.392 (2)	C40—H40A	1.01 (3)
C26—C31	1.3973 (19)	C40—H40B	1.01 (3)
C6—C5	1.3978 (18)	C13—C14	1.510 (3)
C6—C16	1.510 (2)	C13—H13A	0.94 (3)
C5—C10	1.388 (2)	C13—H13B	0.99 (3)
C29—C30	1.395 (2)	C23—H23A	0.95 (3)
C29—H29	0.98 (3)	C23—H23B	0.92 (3)
C41—C42	1.3361 (19)	C20—C19	1.529 (3)
C41—C40	1.508 (2)	C20—H20A	1.00 (3)
C41—C43	1.505 (2)	C20—H20B	1.00 (3)
C37—C38	1.5530 (17)	C43—H43A	0.96 (4)
C37—C42	1.5176 (18)	C43—H43B	0.98 (3)
C37—H37	1.01 (2)	C43—H43C	0.97 (4)
C9—C8	1.397 (2)	C34—C35	1.529 (3)
C9—C10	1.392 (2)	C34—H34A	1.02 (3)
C9—C11	1.507 (2)	C34—H34B	1.04 (3)
C16—C17	1.516 (2)	C14—C15	1.507 (3)

C16—C21	1.550 (2)	C14—H14A	1.06 (4)
C16—H16	0.991 (19)	C14—H14B	0.97 (5)
C8—H8	0.98 (2)	C25—H25A	1.05 (4)
C10—H10	0.98 (2)	C25—H25B	0.94 (3)
C38—C44	1.5131	C25—H25C	0.91 (4)

	(19)		
C38—C39	1.5380 (19)	C45—H45A	1.01 (4)
C38—H38	1.01 (2)	C45—H45B	1.00 (3)
C31—C30	1.388 (2)	C45—H45C	0.91 (4)
C31—H31	0.97 (2)	C46—H46A	1.01 (3)
C42—H42	0.96 (2)	C46—H46B	0.97 (4)
C30—C32	1.516 (2)	C19—H19A	0.95 (3)
C17—C18	1.334 (2)	C19—H19B	0.99 (3)
C17—H17	1.01 (3)	C15—H15A	1.00 (3)
C18—C25	1.506 (3)	C15—H15B	1.03 (4)
C18—C19	1.500 (3)	C15—H15C	0.97 (4)
C44—C45	1.494 (3)	C35—C36	1.517 (4)
C44—C46	1.323 (3)	C35—H35A	0.97 (3)
C21—C22	1.513 (2)	C35—H35B	0.94 (3)
C21—C20	1.532 (2)	C24—H24A	0.96 (3)
C21—H21	0.99 (2)	C24—H24B	0.91 (4)
C22—C23	1.323 (3)	C24—H24C	1.09 (4)
C22—C24	1.507 (3)	C36—H36A	1.00 (3)
C11—C12	1.517 (2)	C36—H36B	0.96 (4)
C11—H11A	1.01 (3)	C36—H36C	1.07 (4)
C7—O2—H2	107.9 (16)	C33—C32—H32B	109.2 (18)
C26—O3—H3	112.3 (18)	H32A—C32—H32B	106 (2)
C28—O4—H4	108.9 (19)	C11—C12—H12A	111.8 (19)
C5—O1—H1	108.4 (18)	C11—C12—H12B	112.7 (19)
O2—C7—C6	120.59 (12)	C13—C12—C11	113.86 (13)
C8—C7—O2	116.69 (12)	C13—C12—H12A	109.4 (18)
C8—C7—C6	122.72 (12)	C13—C12—H12B	108 (2)
C28—C27—C26	116.69 (12)	H12A—C12—H12B	100 (3)

C28—C27—C37	122.01 (11)	C32—C33—H33A	110.4 (16)
C26—C27—C37	121.29 (13)	C32—C33—H33B	105.3 (17)
O4—C28—C27	121.79 (13)	C34—C33—C32	113.65 (17)
O4—C28—C29	115.90 (13)	C34—C33—H33A	108.3 (18)
C29—C28—C27	122.32 (12)	C34—C33—H33B	111.2 (17)
O3—C26—C27	116.85 (12)	H33A—C33—H33B	108 (2)
O3—C26—C31	121.68 (12)	C41—C40—C39	111.66 (12)
C31—C26—C27	121.46 (13)	C41—C40—H40A	110.2 (13)
C7—C6—C16	122.20 (12)	C41—C40—H40B	109.2 (14)
C5—C6—C7	116.12 (12)	C39—C40—H40A	111.0 (13)
C5—C6—C16	121.68 (11)	C39—C40—H40B	110.6 (14)
O1—C5—C6	116.65 (13)	H40A—C40—H40B	103.9 (19)
O1—C5—C10	121.43 (13)	C12—C13—C14	113.65 (15)
C10—C5—C6	121.92 (12)	C12—C13—H13A	109.9 (19)
C28—C29—C30	119.97 (14)	C12—C13—H13B	111.2 (18)
C28—C29—H29	120.1 (13)	C14—C13—H13A	108 (2)
C30—C29—H29	119.9 (13)	C14—C13—H13B	108.2 (17)
C42—C41—C40	121.44 (13)	H13A—C13—H13B	105 (2)
C42—C41—C43	121.36 (14)	C22—C23—H23A	121.3 (17)
C43—C41—C40	117.19 (13)	C22—C23—H23B	124.9 (18)
C27—C37—C38	112.15 (11)	H23A—C23—H23B	114 (2)
C27—C37—H37	106.6 (11)	C21—C20—H20A	106.8

			(18)
C38—C37—H37	107.8 (11)	C21—C20—H20B	109.9 (16)
C42—C37—C27	110.20 (11)	C19—C20—C21	110.68 (15)
C42—C37—C38	111.34 (10)	C19—C20—H20A	111.8 (16)
C42—C37—H37	108.5 (11)	C19—C20—H20B	109.1 (16)
C8—C9—C11	120.68 (13)	H20A—C20—H20B	108 (2)
C10—C9—C8	118.71 (13)	C41—C43—H43A	116 (2)
C10—C9—C11	120.60 (14)	C41—C43—H43B	112.6 (16)
C6—C16—C17	111.32 (12)	C41—C43—H43C	107.7 (19)
C6—C16—C21	112.57 (11)	H43A—C43—H43B	106 (3)
C6—C16—H16	107.6 (12)	H43A—C43—H43C	104 (3)
C17—C16—C21	110.52 (12)	H43B—C43—H43C	111 (3)
C17—C16—H16	105.6 (11)	C33—C34—C35	113.08 (17)
C21—C16—H16	108.9 (12)	C33—C34—H34A	109.5 (14)
C7—C8—C9	119.71 (12)	C33—C34—H34B	108.6 (15)
C7—C8—H8	119.2 (14)	C35—C34—H34A	109.1 (14)
C9—C8—H8	121.1 (14)	C35—C34—H34B	109.3 (14)
C5—C10—C9	120.58 (13)	H34A—C34—H34B	107 (2)
C5—C10—H10	118.7 (13)	C13—C14—H14A	108 (2)
C9—C10—H10	120.7 (13)	C13—C14—H14B	114 (3)
C37—C38—H38	107.4 (11)	C15—C14—C13	114.30 (18)
C44—C38—C37	112.51 (11)	C15—C14—H14A	110 (3)
C44—C38—C39	112.76 (12)	C15—C14—H14B	103 (3)
C44—C38—H38	108.0 (11)	H14A—C14—H14B	107 (4)
C39—C38—C37	108.52 (11)	C18—C25—H25A	110.3 (18)
C39—C38—H38	107.4 (11)	C18—C25—H25B	108.3

			(19)
C26—C31—H31	119.9 (15)	C18—C25—H25C	110 (2)
C30—C31—C26	120.74 (12)	H25A—C25—H25B	115 (3)
C30—C31—H31	119.4 (15)	H25A—C25—H25C	108 (3)
C41—C42—C37	125.11 (12)	H25B—C25—H25C	105 (3)
C41—C42—H42	118.5 (13)	C44—C45—H45A	116 (2)
C37—C42—H42	116.4 (12)	C44—C45—H45B	111 (2)
C29—C30—C32	120.33 (15)	C44—C45—H45C	112 (2)
C31—C30—C29	118.81 (13)	H45A—C45—H45B	106 (3)
C31—C30—C32	120.86 (14)	H45A—C45—H45C	103 (3)
C16—C17—H17	113.6 (14)	H45B—C45—H45C	109 (3)
C18—C17—C16	124.76 (16)	C44—C46—H46A	119 (2)
C18—C17—H17	121.6 (14)	C44—C46—H46B	117 (2)
C17—C18—C25	121.23 (19)	H46A—C46—H46B	124 (3)
C17—C18—C19	121.57 (16)	C18—C19—C20	113.24 (16)
C19—C18—C25	117.16 (18)	C18—C19—H19A	109.6 (18)
C45—C44—C38	118.15 (15)	C18—C19—H19B	109 (2)
C46—C44—C38	120.39 (17)	C20—C19—H19A	110.7 (16)
C46—C44—C45	121.46 (17)	C20—C19—H19B	110.3 (19)
C16—C21—H21	107.7 (13)	H19A—C19—H19B	103 (3)
C22—C21—C16	111.96 (13)	C14—C15—H15A	113 (2)
C22—C21—C20	114.41 (15)	C14—C15—H15B	108 (2)
C22—C21—H21	107.7 (12)	C14—C15—H15C	117 (3)
C20—C21—C16	108.26 (13)	H15A—C15—H15B	105 (3)
C20—C21—H21	106.5 (13)	H15A—C15—H15C	105 (3)
C23—C22—C21	120.27 (16)	H15B—C15—H15C	107 (3)
C23—C22—C24	121.83 (19)	C34—C35—H35A	110.3 (17)
C24—C22—C21	117.87 (18)	C34—C35—H35B	107.5 (19)
C9—C11—C12	113.57 (12)	C36—C35—C34	112.3 (2)
C9—C11—H11A	109.0 (16)	C36—C35—H35A	110.5 (18)
C9—C11—H11B	110.9 (19)	C36—C35—H35B	112 (2)

C12—C11—H11A	109.1 (14)	H35A—C35—H35B	104 (3)
C12—C11—H11B	110 (2)	C22—C24—H24A	110.2 (18)
H11A—C11—H11B	104 (2)	C22—C24—H24B	111 (2)
C38—C39—H39A	110.1 (14)	C22—C24—H24C	106 (2)
C38—C39—H39B	109.3 (14)	H24A—C24—H24B	113 (3)
C40—C39—C38	110.32 (12)	H24A—C24—H24C	106 (3)
C40—C39—H39A	111.6 (13)	H24B—C24—H24C	110 (3)
C40—C39—H39B	109.4 (14)	C35—C36—H36A	111.6 (18)
H39A—C39—H39B	105.9 (19)	C35—C36—H36B	108 (2)
C30—C32—C33	114.85 (14)	C35—C36—H36C	108 (2)
C30—C32—H32A	112.2 (16)	H36A—C36—H36B	110 (3)
C30—C32—H32B	107.4 (17)	H36A—C36—H36C	109 (3)
C33—C32—H32A	106.6 (15)	H36B—C36—H36C	110 (3)

O2—C7—C6—C5	174.74 (12)	C9—C11—C12—C13	−178.47 (15)
O2—C7—C6—C16	−5.95 (19)	C16—C6—C5—O1	2.37 (18)
O2—C7—C8—C9	−175.02 (12)	C16—C6—C5—C10	−178.04 (12)
O3—C26—C31—C30	−179.81 (12)	C16—C17—C18—C25	−178.89 (16)
O4—C28—C29—C30	−179.15 (13)	C16—C17—C18—C19	−1.5 (3)
O1—C5—C10—C9	−177.67 (13)	C16—C21—C22—C23	109.34 (19)
C7—C6—C5—O1	−178.32 (12)	C16—C21—C22—C24	−69.1 (2)
C7—C6—C5—C10	1.27 (18)	C16—C21—C20—C19	−63.94 (19)
C7—C6—C16—C17	59.51 (16)	C8—C7—C6—C5	−5.08 (19)
C7—C6—C16—C21	−65.22 (16)	C8—C7—C6—C16	174.22 (12)
C27—C28—C29—C30	0.7 (2)	C8—C9—C10—C5	−3.1 (2)
C27—C26—C31—C30	1.3 (2)	C8—C9—C11—C12	−55.2 (2)
C27—C37—C38—C44	−67.06 (16)	C10—C9—C8—C7	−0.6 (2)
C27—C37—C38—C39	167.46 (12)	C10—C9—C11—C12	123.46 (16)
C27—C37—C42—C41	−135.63 (17)	C38—C37—C42—C41	−10.5 (2)
C28—C27—C26—O3	−178.98 (11)	C38—C39—C40—C41	50.55 (19)
C28—C27—C26—C31	−0.02 (18)	C31—C30—C32—C33	118.00 (18)
C28—C27—C37—C38	−70.38 (15)	C42—C41—C40—C39	−16.2 (2)
C28—C27—C37—C42	54.26 (16)	C42—C37—C38—C44	168.94 (13)
C28—C29—C30—C31	0.6 (2)	C42—C37—C38—C39	43.46 (16)

C28—C29—C30—C32	−179.24 (13)	C30—C32—C33—C34	−66.3 (2)
C26—C27—C28—O4	178.87 (12)	C17—C16—C21—C22	176.17 (13)
C26—C27—C28—C29	−0.96 (18)	C17—C16—C21—C20	49.14 (16)
C26—C27—C37—C38	109.37 (14)	C17—C18—C19—C20	−11.9 (3)
C26—C27—C37—C42	−125.99 (13)	C44—C38—C39—C40	169.73 (14)
C26—C31—C30—C29	−1.5 (2)	C21—C16—C17—C18	−18.05 (19)
C26—C31—C30—C32	178.27 (13)	C21—C20—C19—C18	44.8 (2)
C6—C7—C8—C9	4.8 (2)	C22—C21—C20—C19	170.46 (16)
C6—C5—C10—C9	2.8 (2)	C11—C9—C8—C7	178.12 (13)
C6—C16—C17—C18	−143.92 (15)	C11—C9—C10—C5	178.21 (13)
C6—C16—C21—C22	−58.66 (16)	C11—C12—C13—C14	−178.8 (2)
C6—C16—C21—C20	174.31 (13)	C39—C38—C44—C45	57.14 (19)
C5—C6—C16—C17	−121.22 (13)	C39—C38—C44—C46	−121.6 (2)
C5—C6—C16—C21	114.05 (13)	C32—C33—C34—C35	−178.50 (17)
C29—C30—C32—C33	−62.2 (2)	C12—C13—C14—C15	−178.5 (2)
C37—C27—C28—O4	−1.37 (19)	C33—C34—C35—C36	177.4 (2)
C37—C27—C28—C29	178.80 (12)	C40—C41—C42—C37	−4.0 (3)
C37—C27—C26—O3	1.26 (18)	C20—C21—C22—C23	−127.02 (19)
C37—C27—C26—C31	−179.78 (11)	C20—C21—C22—C24	54.5 (2)
C37—C38—C44—C45	−66.00 (18)	C43—C41—C42—C37	176.55 (17)
C37—C38—C44—C46	115.25 (19)	C43—C41—C40—C39	163.23 (17)
C37—C38—C39—C40	−64.94 (16)	C25—C18—C19—C20	165.63 (17)